Journal of Medicinal Chemistry

Article

pubs.acs.org/jmc

Synthesis and Biological Evaluation of 4-(Aminomethyl)-1-hydroxypyrazole Analogues of Muscimol as γ-Aminobutyric Acid$_A$ Receptor Agonists

Jette G. Petersen,[†] Rikke Bergmann,[†] Henriette A. Møller,[†] Charlotte G. Jørgensen,[†,‡] Birgitte Nielsen,[†] Jan Kehler,[§] Karla Frydenvang,[†] Jesper Kristensen,[†] Thomas Balle,[#] Anders A. Jensen,[†] Uffe Kristiansen,[†] and Bente Frølund*[,†]

[†]Department of Drug Design and Pharmacology, Faculty of Health and Medical Sciences, University of Copenhagen, Universitetsparken 2, 2100 Copenhagen, Denmark

[‡]Department of Chemistry, University of Oxford, Mansfield Road, OX13TA, United Kingdom

[§]H. Lundbeck A/S, Ottiliavej 9, 2500 Valby, Denmark

[#]Faculty of Pharmacy, The University of Sydney, Camperdown Campus, 2006 New South Wales, Australia

Supporting Information

ABSTRACT: A series of bioisosteric 4-(aminomethyl)-1-hydroxypyrazole (4-AHP) analogues of muscimol, a GABA$_A$ receptor agonist, has been synthesized and pharmacologically characterized at native and selected recombinant GABA$_A$ receptors. The unsubstituted 4-AHP analogue (**2a**) (EC_{50} 19 μM, R_{max} 69%) was a moderately potent agonist at human $\alpha_1\beta_2\gamma_2$ GABA$_A$ receptors, and in SAR studies substitutions in the 3- and/or 5-position were found to be detrimental to binding affinities. Ligand−receptor docking in an $\alpha_1\beta_2\gamma_2$ GABA$_A$ receptor homology model along with the obtained SAR indicate that **2a** and muscimol share a common binding mode, which deviates from the binding mode of the structurally related antagonist series based on 4-(piperidin-4-yl)-1-hydroxypyrazole (4-PHP, **1**). Selectivity for $\alpha_1\beta_2\gamma_2$ over ρ_1 GABA$_A$ receptors was observed for the 5-chloro, 5-bromo, and 5-methyl substituted analogues of **2a** illustrating that even small differences in structure can give rise to subtype selectivity.

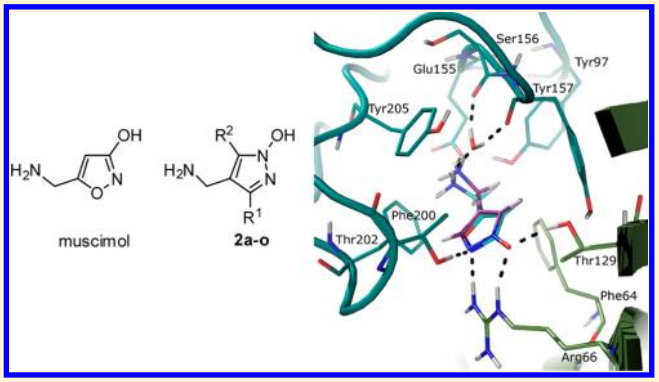

INTRODUCTION

γ-Aminobutyric acid (GABA) is the major inhibitory neurotransmitter in the central nervous system and hence essential for the overall balance between neuronal excitation and inhibition. The GABA neurotransmitter system is known to be implicated in many disorders such as anxiety, epilepsy, mood disorders, insomnia, cognitive disorders, and schizophrenia.[1,2] Dysfunction in the GABA neurotransmitter system has major consequences, and the restoration of the balance between excitation and inhibition is the major aim of therapies affecting the GABAergic system.

The effects of GABA are exerted through the ionotropic GABA$_A$ receptors (GABA$_A$Rs) and the metabotropic GABA$_B$ receptors. The GABA$_A$Rs belong to the Cys-loop receptor superfamily also comprising the nicotinic acetylcholine receptors (nAChRs), 5-HT$_3$ serotonin receptors, and glycine receptors.[3] The receptors are membrane spanning ligand-gated ion channels which, in the case of GABA$_A$Rs, conduct chloride ions. Functional GABA$_A$Rs are pentamers assembled from a pool of 19 different human subunits: α_{1-6}, β_{1-3}, γ_{1-3}, δ, ε, θ, π, and ρ_{1-3}. At least 26 native and mainly heteromeric GABA$_A$R subtypes have been proposed, the $\alpha_1\beta_2\gamma_2$, $\alpha_2\beta_3\gamma_2$, $\alpha_3\beta_3\gamma_2$ combinations being the predominant synaptic receptor subtypes.[4] GABA$_A$Rs composed of ρ_{1-3} subunits assemble as homo- or pseudohomomers and are also known as the GABA$_C$Rs.[5]

Over the years considerable insight into the GABA$_A$R orthosteric binding pocket has been obtained from studies of a range of orthosteric ligands arising from the introduction of conformational restriction and bioisosteric replacement of functional groups in the structure of GABA. Classical ligands include (Figure 1): muscimol,[6] a potent GABA$_A$ agonist isolated from the mushroom *Amanita muscaria*; 4,5,6,7-tetrahydroisoxazolo[5,4-*c*]pyridin-3-ol (THIP),[7] a partial or superagonist depending on subunit composition;[8,9] and 5-(4-piperidyl)-3-isoxazolol (4-PIOL),[10,11] a low efficacy partial agonist at GABA$_A$Rs. These scaffolds have been extensively explored by classical medicinal chemistry, and the results from these studies have been compiled in pharmacophore

Received: October 11, 2012

   dx.doi.org/10.1021/jm301473k | *J. Med. Chem.* XXXX, XXX, XXX−XXX

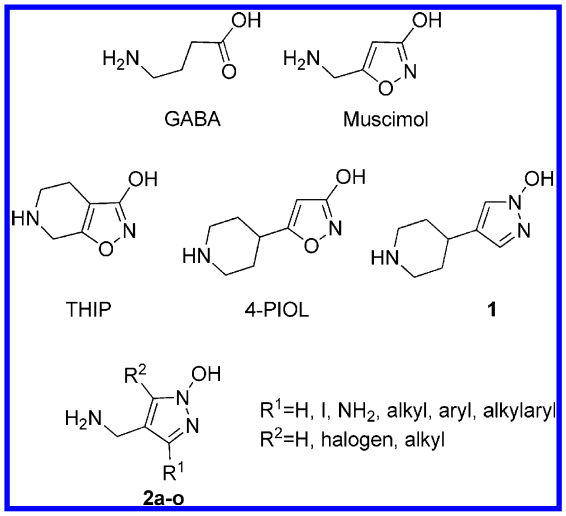

Figure 1. Structures of GABA, muscimol, THIP, 4-PIOL, 4-PHP (**1**), and a general structure of the new 1-hydroxypyrazole compounds **2a–o**.

models.[12,13] In contrast, receptor homology models have had little impact on the drug discovery process, primarily due to a lack of structural information and insufficient sequence identity of available template structures from acetylcholine binding proteins (AChBPs). Progress in protein X-ray crystallography utilizing bacterial ion channels and in particular a glutamate gated channel from the nematode *C. elegans*[14] has changed this picture, and we have recently shown that reliable models of $GABA_A$Rs can be obtained using combinations of the available templates.[15,16]

In our efforts to map the $GABA_A$R orthosteric binding pocket, we have previously established the 1-hydroxypyrazole moiety in 4-(piperidin-4-yl)-1-hydroxypyrazole (4-PHP) (**1**, Figure 1) and analogues thereof as bioisosteric with the 3-hydroxyisoxazole ring of 4-PIOL with respect to the $GABA_A$Rs.[17] All published 4-PHP analogues are moderately to highly potent $GABA_A$R antagonists, and our study revealed cavities in the vicinity of the 3- and 5-position of the 1-hydroxypyrazole ring accommodating large substituents such as phenyl and biphenyl groups.[15,17] On the basis of the successful use of the 1-hydroxypyrazole scaffold for mapping the antagonist binding mode, we here report the synthesis and pharmacological characterization of the comparatively smaller muscimol analogue 4-(aminomethyl)-1-hydroxypyrazole (4-AHP, **2a**) and a series of 4-AHP analogues **2b–o** (Figure 1) as well as two hydroxypyrazol analogues of THIP, **16**, **17**, at the $GABA_A$Rs.

RESULTS

Chemistry. The synthesis of the 4-AHP analogues **2a–o** is illustrated in Schemes 1 and 2. The key intermediate **5** was synthesized from pyrazole following a 5-step procedure.[18–20] Directed ortho lithiation with LDA[21] and subsequent treatment with CBr_4, C_2Cl_6 or MeI gave access to the protected 5-chloro, 5-bromo, and 5-methyl analogues (**6b–d**) (Scheme 1). Compound **6d** was iodinated in the 3-position using iodine monochloride in acetic acid and water[12,17] affording **7** which was subjected to Suzuki cross coupling with methyltrifluoroborate[22] to obtain **8**. All compounds were deprotected with aqueous HBr. The 3-position was accessed through the 3-iodinated intermediate **9** (Scheme 2), which was selectively obtained by refluxing **5** with iodine monochloride in acetic acid and water. Suzuki cross coupling of **9** with arylboronic acids readily afforded the protected phenyl, 3-biphenyl, and 4-biphenyl analogues (**10j,n,o**) in good yields. The protected vinyl analogue **10p** was prepared by reaction with vinyltrifluoroborate salt and subsequent selective reduction of the vinylic double bond using Wilkinson's catalyst[23] affording **10h**. The optimized conditions for the Suzuki cross coupling developed for the formation of **8** were employed for the preparation of 3-alkylsubstituted methyl, benzyl, and phenethyl analogues (**10g,k,l**). The ethylene-4-pyridine analogue **10q** was prepared using standard Heck conditions with vinyl-4-pyridine in excellent yield. Direct amination[24] of the 3-iodinated intermediate **9** with aqueous ammonia under copper-catalysis afforded the 3-amino analogue **10i**. All compounds except **10q** were deprotected with aqueous HBr. Deprotection and hydrogenolysis of the exocyclic double bond of **10q** was accomplished with H_2 and Pd/C.

The synthesis of the intermediate **4** from **3** (Scheme 1) by treating **3** with *i*PrMgCl and reacting the resultant magnesium species with tosylcyanide gave very variable yields (0–82%). Therefore, we investigated palladium-catalyzed aminomethylation using a recently developed cross coupling method with amidomethyltrifluoroborate.[25] Suzuki cross coupling of potassium benzamidomethyl trifluoroborate with the bromo analogue of **3** led us directly to *N*-((1-(benzyloxy)-1*H*-pyrazol-4-yl)methyl)benzamide, the benzamido analogue of intermediate **5**. This method was superior in yield and reduces the number of steps (37% in two steps vs 67% in one step).

Scheme 1[a]

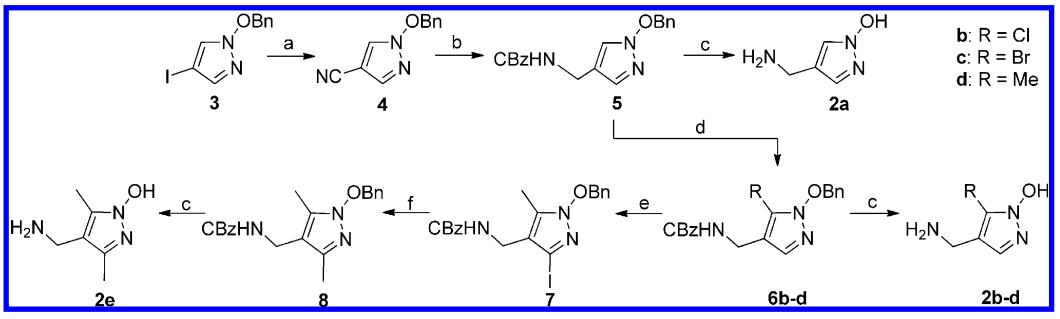

[a]Reagents and conditions: (a) *i*-PrMgCl, TsCN, THF, 0 °C to rt. (b) BnOCOCl, $NaBH_4$, $NiCl_2$, MeOH, 0 °C to rt. (c) 48% aqueous HBr, rt. (d) LDA, THF, −78 °C, C_2Cl_6, CBr_4 or MeI, −78 to −50 °C. (e) ICl, AcOH, H_2O, 85 °C. (f) $MeBF_3K$, $Pd(OAc)_2$, RuPhos, Cs_2CO_3, toluene/H_2O 10:1, 130–140 °C with MW irradiation.

dx.doi.org/10.1021/jm301473k | J. Med. Chem. XXXX, XXX, XXX–XXX

Scheme 2[a]

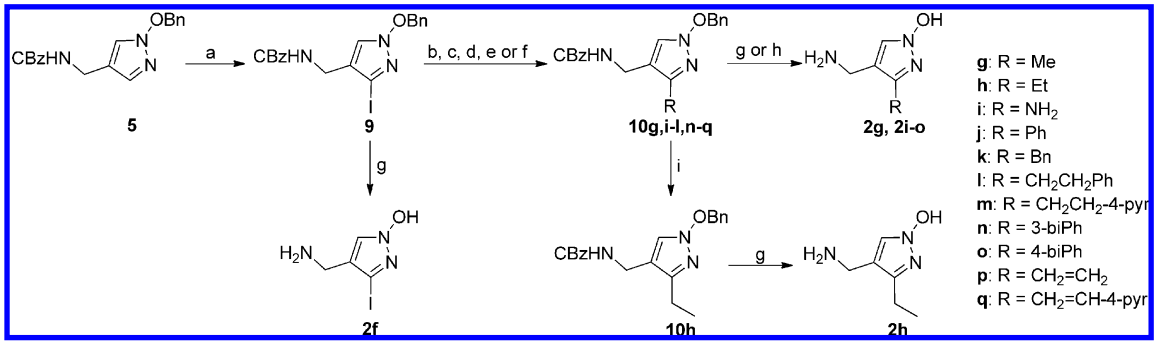

[a]Reagents and conditions: (a) ICl, AcOH, H_2O, 85 °C. For **10j,n,o**: (b) $RB(OH)_2$, $PdCl_2(PPh_3)_2$, K_2CO_3, toluene/EtOH 10:1, 100 °C. For **10p**: (c) CH_2CHBF_3K, $PdCl_2(PPh_3)_2$, K_2CO_3, toluene/EtOH 10:1, 100 °C. For **10g,k,l**: (d) RBF_3K, $Pd(OAc)_2$, RuPhos, Cs_2CO_3, toluene/H_2O 10:1, 100−130 °C with or without MW irradiation. For **10q**: (e) CH_2=CH-4-pyr, $Pd(OAc)_2$, P(o-tol)$_3$, Et_3N, MeCN, 90 °C. For **10i**: (f) 35% aqueous NH_3, 2,4-pentadione, $Cu(acac)_2$, Cs_2CO_3, DMF, 90 °C. For **2g−l,n−o**: (g) 48% aqueous HBr, rt. For **2m**: (h) H_2, Pd/C, MeOH, rt. For **10h**: (i) H_2, $Rh(I)Cl(PPh_3)_3$, MeOH, rt.

However, there is a difference in *N*-protecting groups; whereas the amide protecting group requires harsh acidic conditions for deprotection, the carbamate group allows for different and milder strategies for deprotection. Recently, a cross coupling method utilizing Boc-protected aminomethyltrifluoroborates has been reported[26] giving another option for accessing aminomethylarenes and thereby bypassing the Grignard reaction.

The 1-hydroxypyrazol analogue of THIP, **16**, and the isomeric compound **17** were synthesized from the CBz-protected piperidone **11** (Scheme 3). Treatment of **11** with

Scheme 3[a]

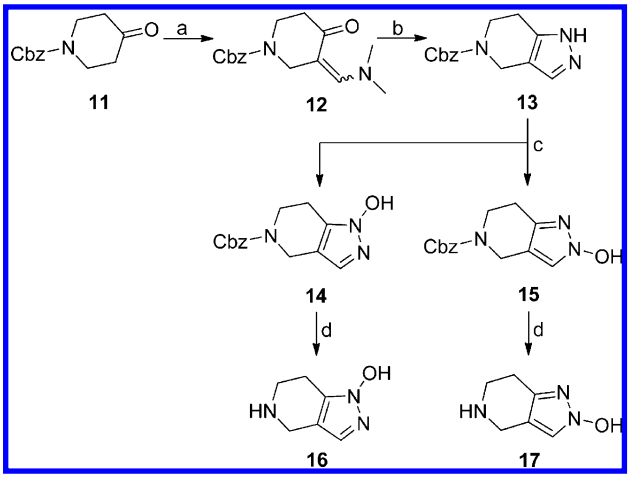

[a]Reagents and conditions: (a) DMF-DMA, 110 °C, (b) N_2H_4, MeOH, reflux, (c) *m*-CPBA, EtOAc, rt, (d) 10% HBr in AcOH, rt.

DMF-DMA afforded **12** which cyclized upon treatment with hydrazine to yield **13**.[27] Oxidation with *m*-CPBA[28] gave rise to two tautomers, **14** and **15**, that were separated using supercritical fluid chromatography, resulting in very low yield, followed by deprotection using HBr in glacial acetic acid. The configuration of the tautomer **17**[29] was assigned as the 2-hydroxypyrazole using X-ray crystallography, and consequently, tautomer **16** was the 1-hydroxypyrazole compound (see Supporting Information for details).

A new and more convergent synthetic strategy to access 4-methylmuscimol, **24**, was developed as opposed to a previously reported route.[30] Compound **24** was synthesized from **18** (Scheme 4), which was prepared from hydroxyurea and

Scheme 4[a]

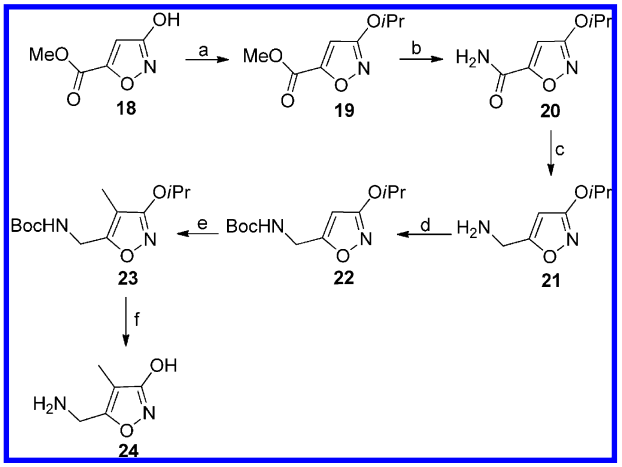

[a]Reagents and conditions: (a) *i*-PrBr, K_2CO_3, DMF, 55 °C, (b) aqueous NH_3, rt, (c) BH_3, THF, rt, (d) Boc_2O, Na_2CO_3, H_2O/dioxane 3:1, 0 °C to rt, (e) *n*-BuLi, MeI, THF, −78 °C, (f) 33% HBr in AcOH, 60 °C.

dimethyl acetylenedicarboxylate.[31] Protection of **18** as the isopropyl ether afforded **19** which was amidated with aqueous ammonia to form amide **20**[32] and reduced with borane to form isopropyl protected muscimol **21**. After Boc-protection of the amine, the methyl group was introduced in the isoxazole 4-position using *n*-butyl lithium and methyl iodide to form **23**. Deprotection with HBr in glacial acetic acid resulted in **24**.

Pharmacology. The binding affinities of the compounds at native $GABA_A$ receptors were measured by displacement of [^{3}H]muscimol in rat membrane preparations. Functional characterization of selected compounds were carried out at the human $\alpha_1\beta_2\gamma_{2S}$ and ρ_1 $GABA_A$ receptors either transiently expressed in tsA201 cells using the FLIPR membrane potential (FMP) blue assay or expressed in HEK 293 cells using whole-cell patch-clamp electrophysiology.

The unsubstituted 4-AHP, **2a**, exhibited binding affinity to the native $GABA_A$Rs in the low micromolar range (Table 1) and a functional profile comparable to those of GABA and muscimol, thus validating the use of the 1-hydroxypyrazole core

dx.doi.org/10.1021/jm301473k | J. Med. Chem. XXXX, XXX, XXX−XXX

Table 1. Pharmacological Data for Reference Compounds GABA, Muscimol, and THIP, 2a−o, 16−17, and 24[a]

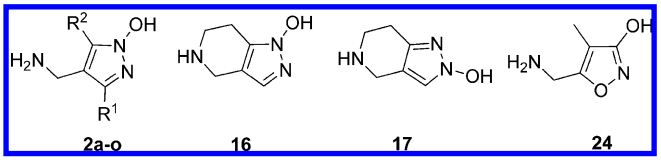

compound	R^1	R^2	[^{3}H]muscimol binding K_i (μM)[b] [pK_i ± SEM]	$\alpha_1\beta_2\gamma_{2S}$ EC_{50} (μM) [pEC_{50} ± SEM]	ρ_1 EC_{50} (μM) [pEC_{50} ± SEM]
GABA			0.049[c]	1.8 [5.75 ± 0.05]	0.27 [6.57 ± 0.02]
muscimol			0.007[d]	0.54 [6.27 ± 0.06]	0.70 [6.16 ± 0.08]
THIP			0.16[e]	14 [4.85 ± 0.03]	100[f]
2a	H	H	0.22 [6.68 ± 0.05]	13 [4.89 ± 0.06]	3.1 [5.51 ± 0.06]
2b	H	Cl	0.63 [6.20 ± 0.03]	29 [4.53 ± 0.05]	>500
2c	H	Br	2.8 [5.56 ± 0.02]	nd	nd
2d	H	Me	15 [4.82 ± 0.04]	>500	>500
2e	Me	Me	>100	nd	nd
2f	I	H	32 [4.50 ± 0.04]	>500	>500
2g	Me	H	68 [4.16 ± 0.08]	nd	nd
2h	Et	H	94 [4.03 ± 0.01]	>500	>500
2i	NH_2	H	>100	nd	nd
2j	Ph	H	>100	>500	>500
2k	Bn	H	>100	nd	nd
2l	CH_2CH_2Ph	H	>100	nd	nd
2m	CH_2CH_2-4-pyr	H	>100	nd	nd
2n	3-biPh	H	17 [4.81 ± 0.10]	>500	>500
2o	4-biPh	H	13 [4.89 ± 0.04]	>300	>500
16			>100	nd	nd
17			>100	nd	nd
24			54 [4.28 ± 0.07]	nd	nd

[a]$GABA_A$ receptor binding affinities at rat synaptic membranes and functional characterization at the human $\alpha_1\beta_2\gamma_{2S}$ and ρ_1 $GABA_A$ receptors transiently expressed in tsA201 cells using the FLIPR membrane potential blue assay. [b]IC_{50} values were calculated from inhibition curves and converted to K_i values. Data are given as the mean [mean pK_i ± SEM] of three to four independent experiments. nd: not determined. [c]From ref 57. [d]Ref 58. [e]Ref 59. [f]Ref 46. Previous measurement on HEK293 cells from the antagonist assay and the value given is IC_{50} (μM).

Table 2. Functional Characteristics of GABA, Muscimol and 2a at the Human $\alpha_1\beta_2\gamma_{2S}$, $\alpha_2\beta_2\gamma_{2S}$, $\alpha_3\beta_2\gamma_{2S}$, $\alpha_5\beta_2\gamma_{2S}$, and ρ_1 $GABA_AR$ Subtypes Transiently Expressed in tsA201 Cells in the FLIPR Membrane Potential Blue Assay[a]

	$\alpha_1\beta_2\gamma_{2S}$ EC_{50} (μM) [pEC_{50} ± SEM]	$\alpha_2\beta_2\gamma_{2S}$ EC_{50} (μM) [pEC_{50} ± SEM]	$\alpha_3\beta_2\gamma_{2S}$ EC_{50} (μM) [pEC_{50} ± SEM]	$\alpha_5\beta_2\gamma_{2S}$ EC_{50} (μM) [pEC_{50} ± SEM]	ρ_1 EC_{50} (μM) [pEC_{50} ± SEM]
GABA	1.8 [5.75 ± 0.05]	0.65 [6.18 ± 0.06]	0.92 [6.04 ± 0.04]	0.11 [6.97 ± 0.12]	0.27 [6.57 ± 0.02]
muscimol	0.54 [6.27 ± 0.06]	0.41 [6.39 ± 0.14]	0.21 [6.67 ± 0.10]	0.054 [7.27 ± 0.11]	0.70 [6.16 ± 0.08]
2a	13 [4.89 ± 0.06]	4.5 [5.35 ± 0.11]	5.6 [5.25 ± 0.10]	0.78 [6.10 ± 0.09]	3.1 [5.51 ± 0.06]

[a]The EC_{50} values are given in μM with pEC_{50} ± SEM values in brackets.

as a bioisosteric replacement for the carboxylic acid in GABA. However, restricting the aminomethyl side chain in a six-membered ring with the THIP analogue **16** and the isomeric compound **17** resulted in loss of affinity. Introduction of chloro, bromo, and methyl substituents in the 5-position of the 1-hydroxypyrazole ring (**2b−d**) also impaired binding affinity. Substitution in the 3-position of the 1-hydroxypyrazole ring followed the trend that larger substituents generated lower binding affinities; there was room for iodo (**2f**) and methyl (**2g**) substituents, but introduction of the more polar amine group (**2i**) and larger ethyl (**2h**), phenyl (**2j**), benzyl (**2k**), phenethyl (**2l**), and 2-(pyridine-4-yl)ethyl (**2m**) groups resulted in loss of affinity.

Introductions of 3- or 4-biphenyl substituents in the 1-hydroxypyrazole 5-position (**2n,o**) resulted in some regain of affinity. The 5- and 3-methyl substituted analogues **2d** and **2g** show some affinity (K_i 15 and 68 μM, respectively), which is lost with the 3,5-dimethyl substituted analogue **2e** (K_i > 100 μM), implying that the tight-fitting binding pocket is not able to accommodate both substituents simultaneously. Introduction of a methyl substituent in the 5-posisiton of 4-AHP (**2d**) gave rise to a significant 10^2 fold decrease in binding affinity compared to the parent compound. In contrast, for the corresponding 4-methyl-muscimol analogue **24**, a more profound 10^4 decrease in binding affinity relative to muscimol was observed.

With respect to functional properties, analogues **2a** and **2c** were characterized as full agonists at both $\alpha_1\beta_2\gamma_{2S}$ and ρ_1 $GABA_ARs$ in the FMP assay (R_{max} values not shown), whereas the biphenyl substituted analogues **2n,o** were devoid of activity at the same receptors at concentrations up to 300−500 μM.

Analogously to muscimol, unsubstituted **2a** displayed agonist activity at all the tested $GABA_AR$ subtypes ($\alpha_1\beta_2\gamma_{2S}$, $\alpha_2\beta_2\gamma_{2S}$, $\alpha_3\beta_2\gamma_{2S}$, $\alpha_5\beta_2\gamma_{2S}$, and ρ_1) (Table 2) in the FMP assay with R_{max} values in the range 77−108% of the maximal response elicited by GABA (data not shown). The EC_{50} values for **2a** at the different subtypes do not reflect any significant subtype selectivity. Interestingly, the 5-substituted 4-AHP analogues

dx.doi.org/10.1021/jm301473k | J. Med. Chem. XXXX, XXX, XXX−XXX

(**2b–d**) showed some degree of selectivity for $\alpha_1\beta_2\gamma_2$ over ρ_1 GABARs in the electrophysiological measurements as opposed to **24** that did not show any activity at concentrations up to 300 μM (Table 3, Figure 2A,B). While 5-chloro, 5-bromo, and 5-methyl analogues showed some activity at the $\alpha_1\beta_2\gamma_{2S}$ receptors, the analogues were inactive at the ρ_1 $GABA_A$Rs at concentrations up to 300 μM. In general, both the FMP assay and electrophysiological measurements showed that **2a** displayed activity at $\alpha_1\beta_2\gamma_2$ and ρ_1 $GABA_A$Rs, whereas **2b–d** displayed reduced activity at the $\alpha_1\beta_2\gamma_2$ $GABA_A$R and no activity at ρ_1 $GABA_A$Rs.

Table 3. Functional Characteristics of Muscimol Analogues 2a–d and 24 at the Human $\alpha_1\beta_2\gamma_2$ and ρ_1 $GABA_A$ Receptors Transiently Expressed in HEK-293 Cells Measured Using Patch-Clamp Electrophysiology[a]

	$\alpha_1\beta_2\gamma_2$		ρ_1	
	EC_{50} (μM)	R_{max}	EC_{50} (μM)	R_{max}
2a	19 [10; 35]	69 [55; 83]	55 [20; 152]	70 [42; 99]
2b	>30 μM	>72%	no response at 300 μM	
2c	>100 μM	>23%	no response at 300 μM	
2d	>10 μM	>64%	no response at 300 μM	
24	no response at 300 μM		no response at 300 μM	

[a]Values are reported as mean (n = 6) and 95% confidence interval (in brackets). R_{max} values are given in % of the maximal response of GABA. Graphic concentration-response relationships on $\alpha_1\beta_2\gamma_2$ $GABA_A$Rs are shown in Supporting Information.

COMPUTATIONAL MODELING

A recently reported full-length model of the $\alpha_1\beta_2\gamma_2$ $GABA_A$ receptor suggesting binding modes of the $GABA_A$R agonists GABA, muscimol, and THIP was used as a starting point for the modeling studies.[16] In the model, GABA is predicted to bridge the β_2 and α_1 subunits, with the acidic moiety forming contacts to α_1Arg66 and hydrogen bonds to β_2Thr202 and α_1Thr129. The ammonium group interacts with β_2Glu155 and hydrogen bonds to the backbone carbonyl of β_2Ser156 and is further stabilized by a π-cation interaction with β_2Tyr205. The hypothesis was rationalized by a large amount of published mutational data. Supported by conformational energy preferences, muscimol was predicted to bind in its global minimum conformation with an aminomethyl side chain torsional angle of around 45°. The amino group is then placed in a slightly different position forming contacts to β2Glu155 and π-cation interactions to two aromatic residues, β2Tyr205 and β2Phe200[16] (Figure 3A, muscimol shown in cyan).

In the present study we used an induced fit docking protocol for compound **2a** similar to that reported for muscimol[16] and obtained essentially the same binding mode (Figure 3A, **2a** shown in purple). In the predicted binding pose of **2a**, substituents in the 3- and 5-positions would clash with either β_2Tyr157 or β_2Phe200 explaining the observed affinity loss of compounds **2b–o** (Figure 3B, **2a** shown in purple and **2d** shown in pink). The affinity decreases with increasing size of the substituent Cl < Br < Me in the 5-position and I < Me < Et in the 3-position supporting the identified binding pose. Finally, when the large 3-biphenyl and 4-biphenyl substituents are inserted in the 3-position some affinity is regained. We have previously shown that there are large hydrophobic pockets flanking the orthosteric binding site on both sides in the antagonist conformation of the receptor.[15,17] However, the 4-AHP scaffold must rotate about 45° in the binding site to allow the biphenyl to pack in the pocket in the subunit interface below the C-loop surrounded by β_2Phe200, α_1Phe45, and α_1Phe64.

DISCUSSION

In the present study, we have expanded the use of the 1-hydroxypyrazole scaffold as a carboxylic acid bioisosteric replacement in the $GABA_A$R agonist area. The 1-hydroxypyrazole scaffold utilized in this study has previously replaced the 3-isoxazolol ring in 4-PIOL,[17] the phenol group in tamoxifen analogues,[33] and the distal carboxylic acid group in (*S*)-glutamic acid[34,35] and aspartic acid[36] analogues. In addition to this bioisosteric property, the 1-hydroxypyrazole scaffold allows for introduction of substituents into the 3- and 5-positions protruding into potentially unexplored areas of the receptor binding pocket. In the study of 4-PIOL analogues, the replacement of the 3-hydroxyisoxazole for 3- and 5-substituted 1-hydroxypyrazoles leads to highly potent $GABA_A$ antagonists, indicating spacious cavities on both sides of the central binding site where the core scaffold binds.

The results of the present study of novel $GABA_A$R agonists show that 1-hydroxypyrazole is a valid bioisosteric replacement, as the 1-hydroxypyrazole analogue of muscimol, **2a**, displays $GABA_A$R affinity in the low micromolar range and pronounced agonist activity at the receptors. We further investigated SAR for 3- and 5-substituted 4-AHP analogues at the $GABA_A$Rs. In contrast to the findings for 4-PHP (**1**)[17] and 4-PIOL,[12,13,37,38] the SAR results for the 5-chloro, 5-bromo, and 5-methyl analogues of **2a** indicate that space is very limited in these areas of the binding pocket. Introduction of iodo, methyl, and ethyl substituents in the 5 position of **2a** also leads to a decrease in affinities as also seen for **16** where the aminomethyl side chain of **2a** has been incorporated into a six-membered ring.

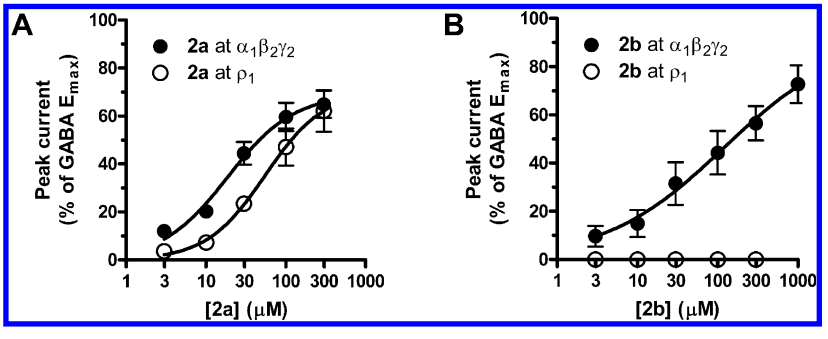

Figure 2. Concentration–response curves for (A) **2a** at $\alpha_1\beta_2\gamma_2$ and ρ_1 $GABA_A$ receptors and (B) **2b** at $\alpha_1\beta_2\gamma_2$ and ρ_1 $GABA_A$ receptors. The $GABA_A$Rs are transiently expressed in HEK-293 cells. Responses were obtained using whole-cell patch-clamp electrophysiology and quantified using the peak currents. The responses are given as % of the maximum response of GABA. Each point represents the mean ± SEM of five to seven different cells.

dx.doi.org/10.1021/jm301473k | J. Med. Chem. XXXX, XXX, XXX–XXX

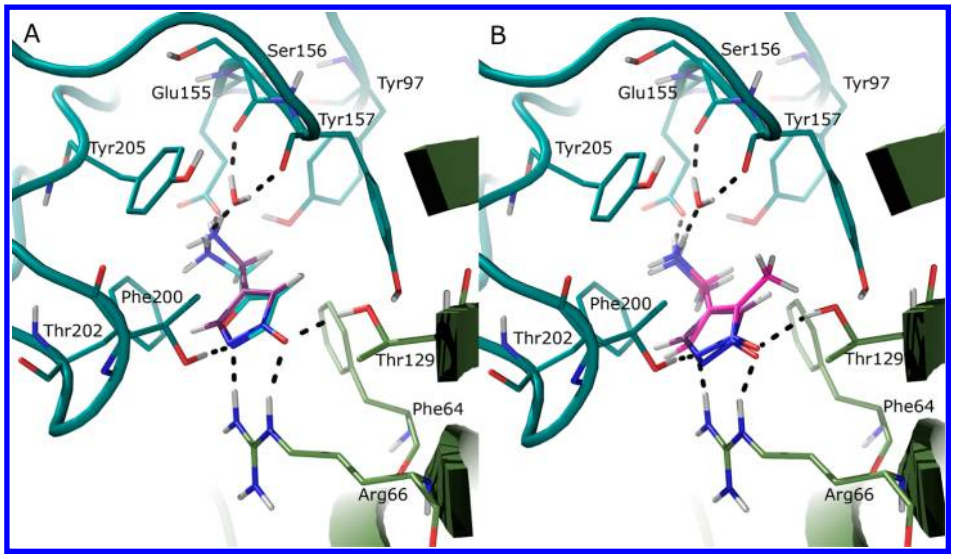

Figure 3. The $GABA_A$ binding site at the interface between the β_2 subunit (teal carbons) and the α_1 subunit (green carbons). (A) The identified docking poses of muscimol (cyan carbons) and **2a** (purple carbons) are nearly identical. Similar interactions are formed between agonist and binding site. A water molecule mediates additional contacts for muscimol and **2a** to the β_2 subunit. (B) The identified docking poses of **2a** (purple carbons) and **2d** (pink carbons). Steric clash of the methyl substituent in the 5-position of the 4-AHP scaffold with β_2Tyr157 can explain the observed reduction of binding affinity of **2d** compared to **2a**.

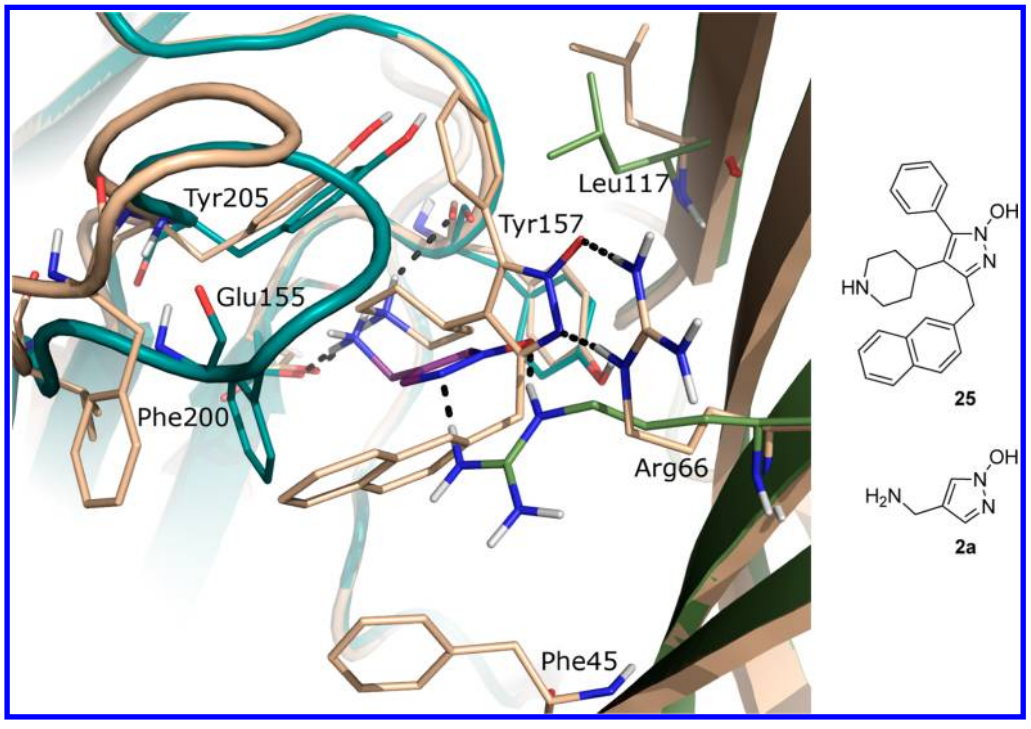

Figure 4. The identified docking poses of **25** (wheat colored carbons) and **2a** (purple carbons). The binding hypothesis of the antagonist **25** was identified previously[15] and requires an open C-loop to accommodate the bulky naphthyl substituent in the 3-position (wheat colored ribbon and protein residues). On the contrary, **2a** forms several contacts to a closed conformation of the C-loop (ribbon and residues in teal). Two different conformations of α_1Arg66 are able to interact with either **2a** (green carbons) or **25** (wheat carbons).

During the progression of the present study, a receptor homology model was developed proposing binding modes for GABA and the $GABA_AR$ agonists muscimol and THIP.[16] Docking of the 4-AHP analogues to this model suggests a common binding mode for muscimol and **2a**, which is supported by parallel SAR of the two series. For muscimol, as well as THIP, it has been shown that introduction of even small aliphatic substituents are detrimental for affinity to the $GABA_ARs$.[39,40]

Although the suggested binding mode for **2a** corresponds well with the SAR, which supports a common binding mode for **2a** and muscimol, it does not explain the 30-fold lower affinity of **2a** compared to muscimol. An understanding of this difference is likely to be found in a combination of conformational energy preferences around the aminomethyl side chain, which is the only flexible part of the molecules, and of pK_a values (4.8 for muscimol[41] and 5.4 for **2a**).

dx.doi.org/10.1021/jm301473k | J. Med. Chem. XXXX, XXX, XXX−XXX

Further SAR differences between muscimol and **2a** are seen by introduction of a methyl group in the 5-position of the 4-AHP core (**2d**) and the corresponding 4-position of muscimol (**24**) which leads to very different changes in binding affinities compared to the respective parent compounds (10^2 vs 10^4 decrease). The docking studies show very similar poses for **2d** and **24** where the methyl groups clash with β_2Tyr157 leading to general affinity loss (Figure 3B). Furthermore, the methyl substituent probably pushes the compounds toward the C-loop. Thereby a small conformational change is enforced in these molecules resulting in an aminomethyl torsional angle closer to 90° to avoid clashes with β_2Tyr157 or the C-loop. This conformational change could be more energetically favorable for **2d** than for **24** explaining the large discrepancy in affinity change for the methyl substituted versus the unsubstituted analogues.

Differing agonist and antagonist binding modes were previously hypothesized in a common 3D-pharmacophore model for $GABA_AR$ agonists and antagonists[12,13] and are supported by homology models.[15,16] Our results indicate a difference between agonist and antagonist binding modes when comparing the 4-AHP analogues to the structurally related 4-PHP analogues. The unsubstituted 4-PHP (**1**, Figure 1) displayed $GABA_AR$ affinity in the low micromolar range, and substitution in the 3- or 5-position of the 1-hydroxylpyrazole core with bulky aromatic groups such as phenyl and biphenyl resulted in potent antagonists at the $GABA_AR$[17] similar to the corresponding 4-PIOL analogues. This is in sharp contrast to the SAR observed for the 4-AHP analogues.

According to pharmacophore and receptor homology models, two distinct low energy conformations of the guanidinium moiety of α_1Arg66 interact with the acidic moiety of **2a** and the corresponding moiety in a 4-PHP analogue as illustrated in Figure 4 for 3,5-disubstituted 4-PHP analogue 3-(naphthalen-2-ylmethyl)-5-phenyl-4-(piperidin-4-yl)-1*H*-pyrazol-1-ol **25**[15] and **2a**. This leads to distinct orientations of the heterocyclic moieties in the binding pocket and can explain the nonparallel SAR for the 4-AHP/4-PHP (**1**) and muscimol/4-PIOL series.

The series of events responsible for receptor activation upon ligand binding is still a matter of debate. AChBPs, the structural surrogates for the ligand binding domain of the Cys-loop receptor superfamily, cocrystallized with different nicotinic agonists and antagonists indicate an important role of C-loop closure upon binding of an agonist.[42] We speculate that for the $GABA_AR$ in the antagonist binding mode there is a limited extent of C-loop closure due to steric hindrance from the bulky aromatic groups. For the small and relatively flat structures of muscimol and 4-AHP full C-loop closure is allowed, which combined with the effect of the flexible α_1Arg66 can rationalize the very limited space for the 4-AHP analogues.

A high degree of similarity exists between the orthosteric binding pockets in the $\alpha_1\beta_2\gamma_2$ $GABA_A$ and the ρ_1 $GABA_A$ receptors, and yet the ρ $GABA_ARs$ have a distinct pharmacology in many respects compared to the other $GABA_ARs$.[43] Unnatural amino acid mutagenesis[44,45] and SAR studies in combination with receptor homology models[46] have revealed slight differences in the orthosteric binding pockets of $\alpha_1\beta_2\gamma_2$ and ρ_1 $GABA_ARs$, and the profiling of compounds from the present study shows that receptor selectivity can be obtained from orthosteric ligands. Future studies are needed to clarify the underlying mechanisms of the observed selectivities.

CONCLUSION

A series of 1-hydroxypyrazole based muscimol analogues have been synthesized and characterized pharmacologically at the $\alpha_1\beta_2\gamma_2$ and ρ_1 $GABA_ARs$. The study identified the 1-hydroxypyrazole scaffold as a bioisosteric replacement for 3-isoxazolol in muscimol within the $GABA_AR$ area. The unsubstituted 4-AHP, **2a**, was shown to be a moderately potent agonist, and SAR studies showed that substitutions in the 3- and 5-positions were detrimental to binding affinities. The observed binding affinities have been addressed based on ligand−receptor docking using a recently developed receptor homology model for the $GABA_AR$. This study and the parallel SAR of muscimol analogues indicate that compound **2a** and muscimol share a common binding mode and network of interactions with the binding pocket leaving no room for substituents. The results support the hypothesized different positions of the acidic heterocycles in the agonists, **2a** and muscimol relative to 4-PHP (**1**) and 4-PIOL. Altogether, these results offer new knowledge about the architecture of the orthosteric binding site in the restricted agonist binding mode and illustrate that small differences in structure are crucial for $GABA_AR$ activity and subtype selectivity, which will have to be clarified in future mutational studies.

EXPERIMENTAL SECTION

Chemistry. *General Procedures.* Compound **4** was prepared according to literature procedures.[18] The preparation of *N*-((1-benzyloxy)-1*H*-pyrazol-4-yl)methylbenzamide is described in Supporting Information. All solvents and reagents were obtained from commercial suppliers and used without further purification. Dry THF was obtained by distillation, and other dry solvents were obtained by storage over 4 Å molecular sieves. All reactions involving air- and/or moisture-sensitive reagents were performed under a nitrogen atmosphere using syringe-septum cap techniques and/or with flame-dried glassware. Analytical thin-layer chromatography (TLC) was carried out using Merck silica gel 60 F254 plates, and the compounds were visualized with UV light (254 nm), $FeCl_3$, ninhydrin, or $KMnO_4$ spraying agents. NMR spectra were recorded on a 300 MHz Varian Mercury Plus spectrometer, a 300 MHz Varian Gemini 2000 spectrometer, or a 500 MHz Bruker Avance DRX500 spectrometer. Dry column vacuum chromatography (DCVC)[47] was performed using Fischer Scientific silica gel 60 (20−45 μm). Flash chromatography (FC) was performed using Merck silica gel 60 (40−63 μm), using Combiflash Companion with a RediSep column with silica gel 60 (35−70 μm), or FlashMaster Personal one column (FP) (ISOLUTE^R SPE Columns) apparatus. Reverse phase FC (RP-FC) was performed using Merck LiChroprep RP-18 (40−63 μm). Details for preparative supercritical flash chromatography (prep. SFC), preparative HPLC (prep. HPLC), analytical HPLC (anal. HPLC) as well as details for pK_a measurement for **2a** can be found in Supporting Information. All microwave reactions were carried out in a glass reactor using a Biotage Initiator instrument. Melting points were determined by OptiMelt from Stanford Research Systems in open capillary tubes and are uncorrected. HRMS was performed by Department of Organic Chemistry, Vrije Universitet Brussel, Belgium. Elemental analysis was performed by Mr. J. Theiner, Department of Physical Chemistry, University of Vienna, Austria, or at the Analytical Research Department, H. Lundbeck A/S, Denmark, and within ±0.4% of the calculated values unless otherwise stated.

*General Procedure for Deprotection (**2a,d-l,n,o**).* The protected compound was dissolved in HBr (48% in H_2O) and stirred at rt for 6 h. The mixture was evaporated under vacuum and re-evaporated from H_2O and toluene followed by recrystallization or column chromatography and recrystallization.

*4-(Aminomethyl)-1H-pyrazol-1-ol Hydrobromide (**2a**).* Deprotection according to the general procedure using **5** (0.26 g, 0.77 mmol). The product was purified by RP-FC and then HBr (48% in H_2O, 1

dx.doi.org/10.1021/jm301473k | J. Med. Chem. XXXX, XXX, XXX−XXX

mL) was added and the mixture was evaporated under vacuum. Recrystallization from MeOH/Et_2O afforded the product as white crystals (0.11 g, 73%). mp > 200 °C. ^1H NMR (CD_3OD): δ 7.88 (s, 1H), 7.56 (s, 1H), 4.11 (s, 2H). ^{13}C NMR (CD_3OD): δ 133.3, 126.0, 112.6, 34.6. Anal. ($C_4H_7N_3O{\cdot}HBr{\cdot}0.1H_2O$) C, H, N.

*4-(Aminomethyl)-5-chloro-1H-pyrazol-1-ol Hydrobromide (**2b**).* **6b** (0.180 g, 0.484 mmol) was dissolved in a mixture of AcOH and HBr (48% in H_2O) and was stirred at 110 °C for 12 h. The mixture was evaporated under vacuum and re-evaporated from H_2O and toluene followed by recrystallization from MeOH/Et_2O affording the product as colorless crystals (57 mg, 52%). mp >220 °C. ^1H NMR (D_2O): δ 7.52 (d, J = 1.8 Hz, 1H), 4.09 (br s, 2H). ^{13}C NMR (CD_3OD): δ 133.6, 122.6, 109.5, 33.8. Anal. ($C_4H_6N_3OCl{\cdot}HBr$) C, H, N.

*4-(Aminomethyl)-5-bromo-1H-pyrazol-1-ol Hydrobromide (**2c**).* Prepared as described for **2b** using **6c** (0.072 g, 0.172 mmol) affording the product as colorless crystals (36 mg, 78%). mp >210 °C. ^1H NMR (CD_3OD): δ 7.52 (s, 1H), 3.93 (s, 2H). ^{13}C NMR ($CDCl_3$): δ 135.1, 113.4, 110.9. Anal. ($C_4H_6N_3OBr{\cdot}1.1HBr$) C, H, N.

*4-(Aminomethyl)-5-methyl-1H-pyrazol-1-ol Hydrobromide (**2d**).* Deprotection according to the general procedure using **6d** (42 mg, 0.12 mmol). The product was purified by prep. HPLC and then HBr (48% in H_2O, 2.5 mL) was added and the mixture was evaporated under vacuum. Recrystallization from MeOH/Et_2O afforded the product as white crystals (11 mg, 44%). mp (decomp) > 184 °C. ^1H NMR (D_2O): δ 7.30 (s, 1H), 4.03 (s, 2H), 2.26 (s, 3H). ^{13}C NMR (CD_3OD) δ 133.1, 132.8, 109.5, 34.5, 8.2. HRMS (ES+) calc. for $C_5H_{10}N_3O$ (MH^+) 128.0818; found 128.0829. Anal. ($C_5H_9N_3O{\cdot}1HBr{\cdot}0.2H_2O$) C, H, N.

*4-(Aminomethyl)-3,5-dimethyl-1H-pyrazol-1-ol Hydrobromide (**2e**).* Deprotection according to the general procedure using **8** (264 mg, 0.72 mmol). The product was purified by prep. HPLC and then HBr (48% in H_2O, 2.5 mL) was added and the mixture was evaporated under vacuum followed by re-evaporation from toluene. Recrystallization from MeOH/Et_2O afforded the product as white crystals (31 mg, 9% over two steps). mp (decomp) > 181 °C. ^1H NMR (D_2O): δ 3.98 (s, 2H), 2.21 (s, 3H), 2.15 (s, 3H). ^{13}C NMR (D_2O): δ 141.5, 134.7, 106.4, 32.6, 10.5, 7.9. HRMS (ES+) calc. for $C_6H_{12}N_3O$ (MH^+) 142.0975; found 142.0981. Anal. ($C_6H_{11}N_3O{\cdot}1.45HBr$) C, H, N.

*4-(Aminomethyl)-3-iodo-1H-pyrazol-1-ol Hydrobromide (**2f**).* Deprotection according to the general procedure using **9** (0.11 g, 0.24 mmol). The product was purified by RP-FC then HBr (48% in H_2O,1 mL) was added and the mixture was evaporated under vacuum. Recrystallization from MeOH/Et_2O afforded the product as white crystals (44 mg, 57%). mp >200 °C. ^1H NMR (CD_3OD): δ 7.67 (s, 1H), 3.94 (s, 2H). ^{13}C NMR (CD_3OD): δ 126.2, 117.6, 92.0, 36.6. Anal. ($C_4H_6IN_3O{\cdot}HBr$) C, H, N.

*4-(Aminomethyl)-3-methyl-1H-pyrazol-1-ol Hydrobromide (**2g**).* Deprotection according to the general procedure using **10g** (96 mg, 0.27 mmol). The product was purified by prep. HPLC and then HBr (33% in AcOH, 0.8 mL) was added and the mixture was evaporated under vacuum. Recrystallization from MeOH/Et_2O afforded the product as white crystals (16 mg, 16% over 2 steps). mp (decomp) > 190 °C. ^1H NMR (D_2O): δ 7.53 (s, 1H), 4.00 (s, 2H), 2.17 (s, 3H).^{13}C NMR (D_2O): δ 142.3, 125.1, 108.7, 33.01, 10.4. HRMS (ES +) calc. for $C_5H_{10}N_3O$ (MH^+) 128.0818; found 128.0824. Anal. ($C_5H_9N_3O{\cdot}1.1HBr$) C, H, N.

*4-(Aminomethyl)-3-ethyl-1H-pyrazol-1-ol Hydrobromide (**2h**).* Deprotection according to the general procedure using **10h** (0.33 g, 0.79 mmol). Recrystallization from MeOH/Et_2O afforded the product as light brown crystals (13 mg, 38%). mp > 200 °C. ^1H NMR (CD_3OD): δ 7.51 (s, 1H), 3.98 (s, 2H), 2.63 (q, J = 7.5 Hz, 2H), 1.24 (t, J = 7.5 Hz, 3H). ^{13}C NMR (CD_3OD): δ 147.9, 125.1, 109.2, 34.0, 20.1, 14.3. Anal. ($C_6H_{11}N_3O{\cdot}1.45HBr$): C, H, N.

*3-Amino-4-(aminomethyl)-1H-pyrazol-1-ol Hydrobromide (**2i**).* Deprotection according to the general procedure using **10i** (89 mg, 0.25 mmol). Recrystallization from MeOH/Et_2O afforded the product as light brown crystals (18 mg, 34%). mp (decomp) > 164 °C. ^1H NMR (D_2O): δ 7.56 (s, 1H), 3.94 (s, 2H). ^{13}C NMR ($CDCl_3$): δ 125.9, 116.7, 91.3, 35.5. Anal. HPLC purity 97% (254 nm).

*4-(Aminomethyl)-3-phenyl-1H-pyrazol-1-ol Hydrobromide (**2j**).* Deprotection according to the general procedure using **10j** (0.33 g, 0.79 mmol). The product was purified by RP-FC and then HBr (48% in H_2O, 1 mL) was added and the mixture was evaporated under vacuum. Recrystallization from MeOH/Et_2O afforded the product as white crystals (73 mg, 34%). mp >200 °C. ^1H NMR (CD_3OD): δ 7.93 (s, 1H), 7.60–7.53 (m, 2H), 7.52–7.37 (m, 3H), 4.19 (s, 2H). ^{13}C NMR (CD_3OD): δ 145.0, 132.2, 129.9, 129.5, 129.2, 126.5, 109.7, 34.6. Anal. ($C_{10}H_{11}N_3O{\cdot}HBr$) C, H, N.

*4-(Aminomethyl)-3-benzyl-1H-pyrazol-1-ol Hydrobromide (**2k**).* Deprotection according to the general procedure using **10k** (137 mg, 0.32 mmol). Recrystallization from MeOH/Et_2O afforded the product as pale yellow crystals (50 mg, 16% over 2 steps). mp (decomp) > 143 °C. ^1H NMR (D_2O): δ 7.57 (s, 1H), 7.34–7.20 (m, 5H), 3.96 (s, 2H), 3.93 (s, 2H).^{13}C NMR (D_2O): δ 144.7, 139.3, 129.3, 128.8, 127.1, 125.4, 108.8, 33.0, 31.6. HRMS (ES+) calc. for $C_{11}H_{14}N_3O$ (MH^+) 204.1131; found 204.1129. Anal. ($C_{11}H_{13}N_3O{\cdot}1.3HBr$) C, H, N.

*4-(Aminomethyl)-3-phenethyl-1H-pyrazol-1-ol Hydrobromide (**2l**).* Deprotection according to the general procedure using **10l** (99 mg, 0.22 mmol). Recrystallization from MeOH/Et_2O afforded the product as pale yellow crystals (23 mg, 10% over 2 steps). mp (decomp) > 188 °C. ^1H NMR (D_2O): δ 7.46 (s, 1H), 7.31–7.22 (m, 3H), 7.13–7.10 (m, 2H), 3.61 (s, 2H), 2.89 (m, 4H).^{13}C NMR (D_2O): δ 144.9, 141.7, 129.2, 129.0, 126.7, 124.6, 109.2, 35.6, 32.7, 27.4. HRMS (ES+) calc. for $C_{12}H_{16}N_3O$ (MH^+) 218.1288; found 218.1289. Anal. ($C_{12}H_{15}N_3O{\cdot}1.1HBr$) C, H, N.

*4-(Aminomethyl)-3-(2-(pyridin-4-yl)ethyl)-1H-pyrazol-1-ol Hydrobromide (**2m**).* **10q** (248 mg, 0.56 mmol) was dissolved in MeOH (5 mL) and Pd/C (10%, 0.124 g) was added. The reaction mixture was stirred at rt under a H_2-atmosphere for 24 h. Additional Pd/C (10%, 0.124 g) was added and stirring was continued for 24 h. The reaction mixture was filtered over Celite and evaporated under vacuum affording the crude product as yellow solid (110 mg, 90%). The crude product was dissolved in HBr (33% in AcOH, 4 mL) and stirred for 5 min at rt. The solvent was evaporated under vacuum affording the product as orange solid (92 mg, 55% over two steps). mp (decomp) > 171 °C. ^1H NMR (D_2O): δ 8.53 (d, J = 5.9 Hz, 2H), 7.78 (d, J = 5.9 Hz, 2H), 7.54 (s, 1H), 3.95 (s, 2H), 3.23 (t, J = 7.3 Hz, 2H), 3.04 (t, J = 7.3 Hz, 2H). ^{13}C NMR (D_2O): δ 163.6, 143.2, 140.6, 127.7, 125.2, 109.0, 95.0, 35.1, 32.7, 25.1. HRMS (ES+) calc. for $C_{11}H_{15}N_4O$ (MH^+) 219.1240; found 219.1243. Anal. HPLC purity 98% (254 nm). Anal. ($C_{11}H_{14}N_4O{\cdot}2HBr{\cdot}1H_2O$) C, H, N.

*4-(Aminomethyl)-3-(biphenyl-3-yl)-1H-pyrazol-1-ol Hydrobromide (**2n**).* Deprotection according to the general procedure using **10n** (0.22 g, 0.45 mmol). The product was purified by RP-FC and then HBr (48% in H_2O, 1 mL) was added and the mixture was evaporated under vacuum. Recrystallization from MeOH/Et_2O afforded the product as white crystals (22 mg, 13%). mp > 200 °C. ^1H NMR (CD_3OD): δ 7.98 (s, 1H), 7.78 (s, 1H), 7.69–7.60 (m, 3H), 7.56–7.51 (m, 2H), 7.47–7.39 (m, 2H), 7.37–7.30 (m, 1H), 4.22 (s, 2H). ^{13}C NMR (CD_3OD): δ 144.9, 142.8, 141.4, 132.8, 130.5, 129.9, 128.6, 128.2, 128.0, 127.9, 127.7, 126.5, 109.9, 34.6. Anal. ($C_{16}H_{15}N_3O{\cdot}HBr{\cdot}1.5H_2O$): C, H, N.

*4-(Aminomethyl)-3-(biphenyl-4-yl)-1H-pyrazol-1-ol Hydrobromide (**2o**).* Deprotection according to the general procedure using **10o** (0.19 g, 0.38 mmol). The product was purified by RP-FC and then HBr (48% in H_2O, 1 mL) was added and the mixture was evaporated under vacuum. Recrystallization from MeOH/Et_2O afforded the product as white crystals (41 mg, 26%). mp > 200 °C. ^1H NMR (CD_3OD): δ 7.82 (s, 1H), 7.76–7.70 (m, 2H), 7.68–7.62 (m, 4H), 7.48–7.41 (m, 2H), 7.38–7.31 (m, 1H), 4.22 (s, 2H). ^{13}C NMR (CD_3OD): δ 144.9, 142.3, 141.5, 132.0, 129.9, 129.6, 128.6, 128.3, 127.8, 125.9, 109.9, 24.8. Anal. ($C_{16}H_{15}N_3O{\cdot}1.8HBr$) C, H, N.

*Benzyl ((1-(benzyloxy)-1H-pyrazol-4-yl)methyl)carbamate (**5**).* To a stirred solution of **4** (6.0 g, 30.1 mmol) in MeOH (20 mL) at 0 °C was added benzyl chloroformate (8.2 mL, 60.2 mmol), nickel chloride hexahydrate (0.72 g, 3.0 mmol), and then $NaBH_4$ (8.0 g, 210 mmol) in small portions over 30 min. The reaction mixture was allowed to reach rt and stirred for 18 h. Diethylenetriamine (3.3 mL, 30.1 mmol) was added and the reaction was left to stir for 0.5 h before it was

dx.doi.org/10.1021/jm301473k | J. Med. Chem. XXXX, XXX, XXX–XXX

evaporated under vacuum. The remaining solid was dissolved in EtOAc (200 mL) and washed with sat. aq. $NaHCO_3$ (2 × 200 mL). The organic phase was dried over $MgSO_4$ and evaporated under vacuum. Purification by DCVC (heptane/EtOAc 100:0 → 60:40) afforded the product as white solid (4.6 g, 45%). mp 92.7−94.7 °C. R_f (heptane/EtOAc 1:1) 0.48. ^{1}H NMR ($CDCl_3$): δ 7.28−7.17 (m, 10H), 7.12 (s, 1H), 6.90 (s, 1H), 5.17 (s, 2H), 5.02 (s, 2H), 4.75 (br s, 1H), 4.05 (d, 2H, J = 5.6 Hz). ^{13}C NMR ($CDCl_3$): δ 156.0, 136.3, 134.6, 132.4, 129.6, 128.6, 128.5, 128.1, 121.8, 116.1, 80.5, 66.8, 35.6.

*Benzyl (1-(benzyloxy)-5-chloro-1H-pyrazol-4-yl)-methylcarbamate (**6b**).* A solution of **5** (0.150 mg, 0.444 mmol) in THF (3 mL) was added dropwise to a solution of LDA (0.49 mL, 2 M in THF) at −78 °C. A solution of C_2Cl_6 (210 mg, 0.89 mmol) in THF (3 mL) was dropwise added to the reaction mixture and stirring was continued for 1 h, and then the temperature was allowed to rise to −50 °C. The mixture was quenched with aq. NH_4Cl (3 mL) and extracted with Et_2O (3 × 5 mL). The combined organic phase was dried over $MgSO_4$ and evaporated under vacuum. Purification by DCVC (heptane/EtOAc 4:1) afforded the product as colorless crystals (170 mg, 99%). ^{1}H NMR ($CDCl_3$): δ 7.29−7.40 (m, 10H), 5.24 (s, 2H), 5.10 (s, 2H), 4.12 (d, J = 5.7 Hz, 2H). ^{13}C NMR ($CDCl_3$): δ 156.1, 136.3, 133.5, 132.9, 130.0, 129.5, 128.6, 128.6, 128.2, 128.2, 116.4, 106.7, 81.2, 67.0, 35.7.

*Benzyl (1-(benzyloxy)-5-bromo-1H-pyrazol-4-yl)-methylcarbamate (**6c**).* Prepared as described for **6b** using **5** (50 mg, 0.148 mmol) in THF (1 mL), LDA (0.165 mL, 2 M in THF) at −78 °C and CBr_4 (98 mg, 0.3 mmol) in THF (1 mL). Purification by DCVC (heptane/EtOAc 4:1) afforded the product as colorless crystals (48 mg, 79%). ^{1}H NMR ($CDCl_3$): δ 7.25−7.42 (m, 10H), 5.26 (s, 2H), 5.11 (s, 2H), 4.15 (d, J = 6.0 Hz, 2H). ^{13}C NMR ($CDCl_3$): δ 156.1, 136.3, 133.5, 132.9, 130.0, 129.5, 128.6, 128.2, 128.1, 116.4, 106.7, 81.2, 67.0, 35.7.

*Benzyl (1-(benzyloxy)-5-methyl-1H-pyrazol-4-yl)-methylcarbamate (**6d**).* Prepared as described for **6b** using **5** (0.150 mg, 0.444 mmol) in THF (3 mL), LDA (0.490 mL, 2 M in THF) at −78 °C and methyliodide (0.060 mL, 0.977 mmol) in THF (3 mL). Purification by DCVC (heptane/EtOAc 4:1) afforded the product as colorless crystals (110 mg, 70%). ^{1}H NMR ($CDCl_3$): δ 7.14−7.32 (m, 11H), 5.19 (s, 2H), 5.07 (s, 2H), 4.07 (d, J = 5.1 Hz, 2H). ^{13}C NMR ($CDCl_3$): δ 156.0, 136.4, 132.1, 129.9, 129.3, 128.5, 128.4, 128.1, 128.0, 119.4, 112.9, 80.1, 66.7, 35.5. 8.0.

*Benzyl ((1-(benzyloxy)-3-iodo-5-methyl-1H-pyrazol-4-yl)methyl)-carbamate (**7**).* To a solution of **6d** (1.12 g, 3.2 mmol) in glacial AcOH (10 mL) a solution of ICl (1.03 g, 6.4 mmol) in glacial AcOH (10 mL) was added followed by H_2O (30 mL). The reaction mixture was stirred at 85 °C for 23 h then cooled to rt. Excess sat. aq. $Na_2S_2O_3$ (30 mL) was added together with H_2O (30 mL), and the mixture was extracted with Et_2O (3 × 60 mL). The organic phase was dried over $MgSO_4$ and evaporated under vacuum. Purification by DCVC (heptane/EtOAc 100:0→80:20) afforded the product as white solid (883 mg, 49%). mp 84.3−86.1 °C. R_f (heptane/EtOAc 1:1) 0.66. ^{1}H NMR ($CDCl_3$): δ 7.40−7.30 (m, 10H), 5.26 (s, 2H), 5.10 (s, 2H), 4.91 (br s, 1H), 4.02 (d, J = 5.7 Hz, 2H), 1.95 (s, 3H).^{13}C NMR ($CDCl_3$): δ 155.9, 136.3, 133.2, 130.0, 129.5, 128.7, 128.5, 128.2, 128.1, 118.0, 91.2, 80.5, 66.8, 36.5, 8.2.

*Benzyl ((1-(benzyloxy)-3,5-dimethyl-1H-pyrazol-4-yl)methyl)-carbamate (**8**).* **7** (300 mg, 0.65 mmol), potassium methyltriflouroborate (687 mg, 3.2 mmol), $Pd(OAc)_2$ (11 mg, 0.05 mmol), RuPhos (45 mg, 0.10 mmol), Cs_2CO_3 (685 mg, 1.9 mmol), and toluene/H_2O (10:1, 3.6 mL) were added to a microwave vial. The vial was purged with N_2, sealed with a cap and heated using microwave irradiation for 5 h at 130 °C. Subsequently, extra reagents were added two times followed by heating using microwave irradiation: (1) potassium methyltriflouroborate (687 mg, 3.2 mmol), $Pd(OAc)_2$ (11 mg, 0.05 mmol) and RuPhos (45 mg, 0.10 mmol), 8 h at 130 °C, (2) potassium methyltriflouroborate (275 mg, 1.3 mmol), $Pd(OAc)_2$ (11 mg, 0.05 mmol) and RuPhos (45 mg, 0.10 mmol), 3 h at 140 °C. H_2O (10 mL) was added and the reaction mixture was extracted with EtOAc (3 × 10 mL). The organic phase was dried over $MgSO_4$ and evaporated under vacuum. Purification by DCVC (heptane/EtOAc 100:0 → 70:30) afforded a mixture of the product and dehalogenated starting material (6:4) as yellow oil. R_f (heptane/EtOAc 1:1) 0.45. The mixture was used directly for the formation of **2e**.

*Benzyl ((1-(benzyloxy)-3-iodo-1H-pyrazol-4-yl)methyl)carbamate (**9**).* Prepared as described for **7** using **5** (2.06 g, 6.1 mmol). Purification by DCVC (heptane/EtOAc 100:0 → 80:20) afforded the product as white solid (2.03 g, 72%). mp 57.2−59.2 °C. R_f (heptane/EtOAc 1:1) 0.63. ^{1}H NMR ($CDCl_3$): δ 7.39−7.31 (m, 10 H), 6.97 (s, 1H), 5.28 (s, 2H), 5.10 (s, 2H), 4.97 (br s, 1H), 4.04 (d, 2H, J = 6.2 Hz). ^{13}C NMR ($CDCl_3$): δ 156.5, 136.7, 133.7, 130.1, 129.9, 129.2, 129.0, 128.7, 128.6, 124.3, 121.5, 90.9, 81.6, 67.3, 37.5.

*Benzyl ((1-(benzyloxy)-3-methyl-1H-pyrazol-4-yl)methyl)-carbamate (**10g**).* Prepared as described for **8** using **9** (300 mg, 0.65 mmol), potassium methyltrifluoroborate (395 mg, 3.2 mmol), $Pd(OAc)_2$ (10.9 mg, 0.05 mmol), RuPhos (45.3 mg, 0.10 mmol), Cs_2CO_3 (685 mg, 1.9 mmol) and toluene/H_2O (10:1, 3.9 mL) with heating for 2 h at 130 °C. Subsequently, extra reagents were added followed by heating using microwave irradiation: potassium methyltrifluoroborate (395 mg, 3.2 mmol), $Pd(OAc)_2$ (10.9 mg, 0.05 mmol), RuPhos (45.3 mg, 0.10 mmol), 8 h at 130 °C. Purification by DCVC (heptane/EtOAc 100:0 → 80:20) afforded a mixture of the product and dehalogenated starting material (9:1). R_f (heptane/EtOAc 1:1) 0.45. The product was used directly for the formation of **2g**.

*Benzyl (1-(benzyloxy)-3-ethyl-1H-pyrazol-4-yl)methylcarbamate (**10h**).* **10p** (65 mg, 0.18 mmol) was dissolved in dry MeOH (5 mL) and $Rh(I)Cl(PPh_3)_3$ (Wilkinson's catalyst) (8 mg, 9 μmol) was added. Hydrogen was flushed through the solution, and the reaction mixture was stirred at rt for 15 h. Extra $Rh(I)Cl(PPh_3)_3$ (8 mg, 9 μmol) was added, and hydrogen was applied once more and the reaction mixture was stirred for another 15 h. The mixture was evaporated under vacuum and purification by DCVC afforded the product as clear oil (57 mg, 87%). ^{1}H NMR ($CDCl_3$): δ 7.40−7.26 (10H, m), 6.91 (1H, s), 5.22 (2H, s), 5.10 (2H, s), 4.80 (1H, br s), 4.11 (2H, d, J = 5.3 Hz), 2.60 (2H, q, J = 7.6 Hz), 1.24 (3H, t, J = 7.6 Hz). ^{13}C NMR ($CDCl_3$): δ 156.0, 146.5, 136.5, 134.0, 129.7, 129.2, 128.7, 128.6, 128.2, 128.1, 122.7, 112.5, 80.5, 66.9, 34.8, 19.8, 14.1.

*Benzyl ((3-amino-1-(benzyloxy)-1H-pyrazol-4-yl)methyl)-carbamate (**10i**).* **9** (200 mg, 432 mmol), $Cu(acac)_2$ (11 mg, 43.2 mmol), Cs_2CO_3 (281 mg, 863 mmol) and DMF (2.2 mL) were added to a vial and the solution was degassed with N_2. 2,4-Pentadione and ammonia solution (35% in H_2O, 0.13 mL) were added and the reaction mixture was stirred at 90 °C for 1 h. CH_2Cl_2 (10 mL) was added and the mixture was filtered through Celite. The filtercake was washed with CH_2Cl_2 and the filtrate washed with H_2O (2 × 8 mL). The aqueous phases were combined and extracted with CH_2Cl_2 (10 mL). The organic phases were combined, dried over $MgSO_4$ and evaporated under vacuum. Purification by DCVC (heptane/EtOAc 100:0 → 80:20) afforded the product as clear oil (106 mg, 70%). R_f (heptane/EtOAc 1:1) 0.64. IR: 3419, 3321, 3032, 2948, 1701 cm^{-1}. ^{1}H NMR ($CDCl_3$): δ 7.39−7.31 (m, 10H), 6.97 (s, 1H), 5.28 (s, 2H), 5.10 (s, 2H), 4.97 (br s, 1H), 4.02 (d, J = 5.9 Hz, 2H). ^{13}C NMR ($CDCl_3$): δ 156.0, 136.2, 133.2, 129.6, 129.4, 128.7, 128.5, 128.1, 128.0, 123.8, 121.0, 90.4, 81.1, 66.8, 37.0.

*Benzyl (1-(benzyloxy)-3-phenyl-1H-pyrazol-4-yl)-methylcarbamate (**10j**).* **9** (0.51 g, 1.1 mmol) and phenylboronic acid 97% (0.27 g, 2.2 mmol) were dissolved in toluene/EtOH (10:1, 22 mL). Aqueous K_2CO_3 (3 M, 0.72 mL) and $PdCl_2(PPh)_2$ (40 mg, 0.06 mmol) were added. The reaction mixture was stirred at 100 °C for 20 h and then cooled to rt. Et_2O (30 mL) was added and the mixture was washed with H_2O (30 mL), NaOH (1 M, 2 × 30 mL), and H_2O (30 mL). The organic phase was dried over $MgSO_4$ and evaporated under vacuum. Purification by DCVC (heptane/EtOAc 3:1) afforded the product as clear oil. (0.38 g, 84%). ^{1}H NMR ($CDCl_3$): δ 7.62−7.56 (m, 2H), 7.46−7.30 (m, 13H), 7.09 (s, 1H), 5.33 (s, 2H), 5.10 (s, 2H), 4.81 (br s, 1H), 4.32 (d, J = 5.3 Hz, 2H). ^{13}C NMR ($CDCl_3$): δ 156.1, 143.7, 136.4, 133.8, 132.7, 129.7, 129.4, 128.7, 128.6, 128.2, 128.1, 127.9, 127.7, 123.8, 113.3, 80.8, 66.9, 35.7.

*Benzyl ((3-benzyl-1-(benzyloxy)-1H-pyrazol-4-yl)methyl)-carbamate (**10k**).* Prepared as described for **8** using **9** (518 mg, 1.1 mmol), potassium benzyltrifluoroborate (554 mg, 2.8 mmol),

$Pd(OAc)_2$ (19 mg, 0.08 mmol), RuPhos (78 mg, 0.17 mmol), Cs_2CO_3 (1.18 g, 3.4 mmol), and toluene/H_2O (10:1, 6.2 mL) with heating for 4 h at 130 °C. Subsequently, extra reagents were added followed by heating using microwave irradiation: potassium benzyltriflouroborate (305 mg, 1.6 mmol), $Pd(OAc)_2$ (19 mg, 0.08 mmol) and RuPhos (78 mg, 0.17 mmol), 4 h at 130 °C. Purification by DCVC (heptane/EtOAc 100:0 → 80:20) afforded the product as yellow oil contaminated by phosphine ligand (~7:3 distribution) (156 mg, 33%). R_f (heptane/EtOAc 1:1) 0.69. ^{1}H NMR ($CDCl_3$): δ 7.27−7.09 (m, 15H), 6.86 (s, 1H), 5.17 (s, 2H), 4.94 (s, 2H), 4.23 (br s, 1H), 3.88−3.85 (m, 4H), 1.25−1.19 (m, 6H, impurity), 0.83−0.79 (m, 4H, impurity). ^{13}C NMR ($CDCl_3$): δ 155.8, 143.6, 139.4, 133.7, 129.6, 129.2, 128.5, 128.5, 128.4, 128.0, 127.9, 126.3, 123.3, 113.3, 80.4, 66.5, 34.6, 32.9, 31.8, 29.0, 22.7, 14.1.

*Benzyl ((1-(benzyloxy)-3-phenethyl-1H-pyrazol-4-yl)methyl)-carbamate (**10l**).* Prepared as described for **8** using **9** (350 mg, 0.76 mmol), potassium phenethyltrifluoroborate (408 mg, 1.9 mmol), $Pd(OAc)_2$ (13 mg, 0.06 mmol), RuPhos (53 mg, 0.11 mmol), Cs_2CO_3 (800 mg, 2.3 mmol), and toluene/H_2O (10:1, 4.2 mL) with heating at 100 °C on oil bath for 19 h. No extra addition of reagents. Purification by DCVC (heptane/EtOAc 100:0 → 85:15) afforded the product as clear oil contaminated by phosphine ligand (~75:25 distribution) (99 mg, 30%). R_f (heptane/EtOAc 1:1) 0.64. ^{1}H NMR ($CDCl_3$): δ 7.27−7.02 (m, 15H), 6.76 (s, 1H), 5.13 (s, 2H), 4.96 (s, 2H), 4.17 (br s, 1H), 3.77 (d, J = 5.6 Hz, 2H), 2.87 (t, J = 6.7 Hz, 2H), 2.78 (t, J = 6.7 Hz, 2H), 1.19 (s, 5H, impurity), 0.80 (m, 3H, impurity). ^{13}C NMR ($CDCl_3$): δ 155.8, 143.9, 141.3, 133.8, 133.7, 129.5, 129.1, 128.6, 128.5, 128.5, 128.4, 128.3, 128.2, 128.0, 127.9, 126.1, 126.0, 122.5, 113.4, 80.4, 66.6, 36.1, 34.5, 31.9, 29.0, 29.0, 28.2, 22.6, 14.1.

*Benzyl (1-(benzyloxy)-3-(biphenyl-3-yl)-1H-pyrazol-4-yl)-methylcarbamate (**10n**).* Prepared as described for compound **10j** using **9** (0.25 g, 0.54 mmol), 3-biphenylboronic acid (0.25 g, 1.2 mmol), toluene/EtOH (10:1, 11 mL), aqueous K_2CO_3 (3 M, 0.42 mL), and $PdCl_2(PPh)_2$ (22 mg, 0.03 mmol). Purification by DCVC (heptane/EtOAc 3:1) afforded the product as clear oil (0.22 g, 82%). ^{1}H NMR ($CDCl_3$): δ 7.88 (s, 1H), 7.71−7.56 (m, 4H), 7.53−7.43 (m, 3H), 7.43−7.28 (m, 11H), 7.12 (s, 1H), 5.35 (s, 2H), 5.11 (s, 2H), 5.04 (br s, 1H), 4.37 (d, J = 5.3 Hz, 2H). ^{13}C NMR ($CDCl_3$): δ 156.1, 143.6, 141.7, 140.9, 136.4, 133.7, 133.2, 129.7, 129.4, 129.2, 128.8, 128.7, 128.6, 128.2, 128.1, 127.5, 127.3, 126.7, 126.6, 123.8, 113.4, 80.8, 66.9, 35.8.

*Benzyl (1-(benzyloxy)-3-(biphenyl-4-yl)-1H-pyrazol-4-yl)-methylcarbamate (**10o**).* Prepared as described for compound **10j** using **9** (0.27 g, 0.58 mmol), 4-biphenylboronic acid (0.24 g, 1.2 mmol), toluene/EtOH (10:1, 11 mL), aqueous K_2CO_3 (3 M, 0.38 mL), and $PdCl_2(PPh)_2$ (20 mg, 0.03 mmol). Purification by DCVC (heptane/EtOAc 3:1) afforded the product as clear oil (0.23 g, 81%). ^{1}H NMR ($CDCl_3$): δ 7.74−7.61 (m, 6H), 7.52−7.43 (m, 2H), 7.43−7.28 (m, 11H), 7.10 (s, 1H), 5.35 (s, 2H), 5.12 (s, 2H), 4.93 (br s, 1H), 4.37 (d, J = 5.3 Hz, 2H). ^{13}C NMR ($CDCl_3$): δ 156.1, 143.3, 140.6, 136.4, 133.7, 131.7, 129.7, 129.4, 128.9, 128.8, 128.6, 128.3, 128.2, 128.0, 127.5, 127.4, 127.1, 123.9, 113.3, 80.8, 66.9, 35.9.

*Benzyl (1-(benzyloxy)-3-vinyl-1H-pyrazol-4-yl)methylcarbamate (**10p**).* Prepared as described for compound **10j** using **9** (200 mg, 0.42 mmol), potassium vinyl trifluoroborate (110 mg, 0.84 mmol), toluene/EtOH (10:1, 22 mL), aqueous K_2CO_3 (3 M, 0.38 mL), and $PdCl_2(PPh)_2$ (15 mg, 0.02 mmol). Purification by DCVC (heptane/EtOAc 3:1) afforded the product as clear oil (74 mg, 48%). ^{1}H NMR ($CDCl_3$): δ 7.40−7.27 (m, 10H), 6.94 (s, 1H), 6.63 (dd, J = 17.6 Hz, J = 11.1 Hz, 1H), 5.79 (d, J = 17.6 Hz, 1H), 5.31 (d, J = 11.1 Hz, 1H), 5.25 (s, 2H), 5.10 (s, 2H), 4.94 (br s, 1H), 4.20 (d, J = 5.3 Hz, 2H). ^{13}C NMR ($CDCl_3$): δ 156.0, 141.6, 136.4, 133.4, 129.7, 129.3, 128.7, 128.6, 128.2, 128.1, 126.7, 123.3, 116.1, 113.7, 80.7, 66.9, 35.0.

*(E)-Benzyl ((1-(benzyloxy)-3-(2-(pyridin-4-yl)vinyl)-1H-pyrazol-4-yl)methyl)carbamate (**10q**).* **9** (500 mg, 1.1 mmol), 4-vinylpyridine (0.35 mL, 3.2 mmol), $Pd(OAc)_2$ (73 mg, 0.32 mmol), tri(o-tolyl)phosphine (329 mg, 1.1 mmol), and triethylamine (0.03 mL, 21.6 mmol) were dissolved in MeCN (5 mL) and heated at 90 °C for 2.5 h. The reaction mixture was cooled to rt and added sat. aq. NH_4Cl (10 mL) followed by extraction with EtOAc (3 × 10 mL). The combined organic phases were washed with H_2O (10 mL) and brine (10 mL). The organic phase was dried over $MgSO_4$ and evaporated under vacuum. Purification by DCVC (heptane/EtOAc 100:0 → 0:100) afforded the product as yellow crystals (432 mg, 89%). R_f (heptane/EtOAc 1:1) 0.08. ^{1}H NMR ($CDCl_3$): δ 8.45 (d, J = 5.9 Hz, 2H), 7.30−7.22 (m, 12 H), 7.14 (d, J = 16.1 Hz, 1H), 7.04 (d, J = 16.1 Hz, 1H), 6.88 (s, 1H), 5.22 (s, 2H), 5.03 (s, 2H), 4.83 (br s, 1H), 4.20 (d, 2H).^{13}C NMR ($CDCl_3$): δ 156.4, 150.5, 144.9, 141.1, 136.7, 133.9, 130.1, 129.8, 129.1, 129.0, 128.6, 128.4, 127.7, 124.1, 122.5, 121.2, 115.6, 81.2, 67.3, 35.1.

*N-Benzyloxycarbonyl-3-(dimethylaminomethylene)-4-piperidone (**12**).* **11** (5.0 g, 21.4 mmol) was dissolved in *N*,*N*-dimethylformamide dimethyl acetal (20 mL) and refluxed at 110 °C for 2 h. The reaction mixture was evaporated under vacuum and purified by FC (EtOAc/EtOH 1:0→ 10:1) affording the product (2.7 g, 44%). R_f (EtOAc) 0.13. ^{1}H NMR ($CDCl_3$): δ 7.49 (s, 1H), 7.29−7.36 (m, 5H), 5.16 (s, 2H), 4.61 (s, 2H), 3.69 (t, J = 7 Hz, 2H), 3.11 (br s, 6H), 2.46 (br s, 2H). ^{13}C NMR ($CDCl_3$): δ 194.3, 155.4, 149.3, 136.8, 128.6, 128.1, 127.9, 100.8, 67.29, 43.6, 42.3, 41.2, 37.5.

*4,5,6,7-Tetrahydropyrazolo[4,5-c]pyridine-5-carboxylic Acid Benzyl Ester (**13**).* **12** (12.5 g, 43 mmol) was dissolved in MeOH (200 mL). Hydrazine hydrate (2.5 mL, 52 mmol) was added and the reaction was refluxed for 2 h. The reaction mixture was evaporated under vacuum and purified by FC (petroleum ether/EtOAc 1:1 → 0:1) affording the product (9.2 g, 82%). R_f(EtOAc) 0.4. ^{1}H NMR ($CDCl_3$) δ 7.25−7.36 (m, 6H), 5.16 (s, 2H), 4.55 (br s, 2H), 3.76 (br s, 2H), 2.77 (br s, 2H).

*1-Hydroxy-4,5,6,7-Tetrahydropyrazolo[4,5-c]pyridine-5-carboxylic Acid Benzyl Ester (14) and 1-Hydroxy-3,4,5,6-Tetrahydropyrazolo[4,3-c]pyridine-5-carboxylic Acid Benzyl Ester (**15**).* **13** (9.2 g, 36 mol) was dissolved in EtOAc (100 mL) followed by the addition of *m*-CPBA (70−75%, 8.1 g, 34 mol). The reaction mixture was stirred for 6 days at rt and then evaporated under vacuum. The purification was performed over several steps, and after every purification the fractions containing product were collected and evaporated under vacuum: The mixture was purified by FC (1% AcOH in toluene/EtOAc 8:1 → 2:1), then redissolved in Et_2O/EtOAc (2:1 mixture) and washed with 1 N HCl two times (which should remove starting material **13**), H_2O and brine. The organic phase was dried with $MgSO_4$ and evaporated under vacuum giving 2.22 g (bumps very easily) of a crude mixture still containing starting material **13**. The mixture was purified again using FC (petroleum ether/EtOAc 1:1 → 0:1) giving 1.43 g of a crude mixture of the two products visualized by NMR (NMR: two products, LC-MS one peak). Prep. SFC resulted in three batches with diethylamine present (579 mg of "impure **14**", 171 mg of "impure **15**", 99 mg of "mix of **14** and **15**)"). Purification by FC (EtOAc/petroleum ether 3:1) of "impure **14**" and "impure **15**" gave pure **14** (278 mg, 3%) and pure **15** (109 mg, 1%). **14:** ^{1}H NMR ($CDCl_3$): δ 11.35 (0.9H), 7.30−7.34 (m, 5H), 6.87 (br s, 1H), 5.13 (s, 2H), 4.45 (s, 2H), 3.73 (br s, 2H), 2.60 (br s, 2H). **15:** ^{1}H NMR ($CDCl_3$): δ 10.62 (0.3H), 7.30−7.34 (m, 5H), 7.11 (br s, 1H), 5.14 (s, 2H), 4.46 (s, 2H), 3.73 (br s, 2H), 2.60 (br s, 2H).

*4,5,6,7-Tetrahydropyrazolo[4,5-c]pyridin-1-ol Hydrobromide (**16**).* **14** (258 mg, 0.9 mmol) was dissolved in HBr (10% in AcOH) and stirred at rt for 15 min. The mixture was evaporated under vacuum, triturated with Et_2O, followed by recrystallization from EtOH/Et_2O affording the product as colorless crystals (118 mg, 57%). ^{1}H NMR (DMSO-d_6): δ 12.20 (s, 1H), 8.88 (br s, 2H), 7.08 (s, 1H), 4.11 (s, 2H), 3.39 (br s, 2H), 2.85 (t, J = 6 Hz, 2H). Anal. ($C_6H_9N_3O$·HBr) C, H, N.

*3,4,5,6-Tetrahydro-pyrazolo[4,3-c]pyridin-1-ol Hydrobromide (**17**).* Prepared as described for **16** using **15** (109 mg, 0.4 mmol) affording the product as colorless crystals (58 mg, 66%). ^{1}H NMR (DMSO-d_6): δ 12.36 (s, 1H), 8.80 (br s, 2H), 7.49 (s, 1H), 4.09 (s, 2H), 3.39 (t, J = 7 Hz, 2H), 2.79 (t, J = 6 Hz, 2H). Anal. ($C_6H_9N_3O$·HBr) C, H, N.

*3-Isopropoxy-5-(methoxycarbonyl)-isoxazol (**19**).* A mixture of **18** (2.0 g, 13.97 mmol) and K_2CO_3 (2.12 g, 15.37 mmol) in dry DMF (25 mL) was stirred for 1 h at 60 °C. Isopropyl bromide (1.96 mL, 21.0 mmol) was added and the mixture was stirred overnight at 55 °C.

dx.doi.org/10.1021/jm301473k | J. Med. Chem. XXXX, XXX, XXX−XXX

Water (40 mL) was added and the aqueous phase was extracted with Et_2O (3 × 25 mL). The combined organic phases were dried over $MgSO_4$, filtered, and evaporated under vacuum. Purification by DCVC (heptane/EtOAc 5:1) afforded the product as colorless oil (2.2 g, 88%). ^1H NMR ($CDCl_3$): δ 6.50 (s, 1H), 4.94 (hep, J = 6.0 Hz, 1H), 3.94 (s, 3H), 1.40 (d, J = 6.0 Hz, 6H). Spectral data were in agreement with the literature.[32]

*5-Carbamoyl-3-isopropoxyisoxazole (**20**).* A mixture of **19** (3.5 g, 18.9 mmol) and aqueous ammonia (25%) was stirred overnight at rt. The reaction mixture was evaporated under vacuum and evaporated twice with water and twice with toluene affording the product as colorless crystals (3.0 g, 94%). ^1H NMR (CD_3OD): δ 6.57 (s, 1H), 4.88−4.93 (m, 1H), 1.42 (d, J = 6.6 Hz, 6H). Spectral data were in agreement with the literature.[32]

*5-Aminomethyl-3-isopropoxyisoxazole (**21**).* A solution of **20** (3.0 g, 17.6 mmol) in dry THF (50 mL) was slowly added a solution of borane in THF (26.4 mL, 1 M). The reaction mixture was stirred overnight at rt. 4N HCl (aq) was added to pH 1 followed by stirring for 1 h and evaporation under vacuum. The remaining solid was suspended in water and 5 N NaOH (aq) was added to pH 12. The aqueous mixture was extracted with Et_2O (3 × 50 mL) and the combined organic phase was dried over $MgSO_4$ and evaporated under vacuum affording the product as yellow oil (2.0 g, 72%). ^1H NMR ($CDCl_3/CD_3OD$): δ 5.78 (1H, s), 4.80 (hep, J = 6.0 Hz, 1H), 3.82 (s, 2H), 3.62 (br s, 2H), 1.37 (d, J = 6.0 Hz, 6H).

*5-(tert-Butyloxycarbonyl)aminomethyl-3-isopropoxyisoxazole (**22**).* To an ice cold solution of Na_2CO_3 (0.679 g, 6.4 mmol) in water (2 mL) was slowly added a solution of **21** (0.5 g, 3.2 mmol) in dioxane/H_2O (3:1, 8 mL) over 1 h at 0 °C. A solution of di-*tert*-butyl dicarbonate (0.77 g, 3.5 mmol) in dioxane (2 mL) was added dropwise, and the reaction mixture was stirred overnight at rt. Dioxane was evaporated under vacuum and the aqueous phase was extracted with Et_2O (3 × 20 mL). The combined organic phases were dried over $MgSO_4$ and evaporated under vacuum. Purification by DCVC (heptane/EtOAc 4:1) afforded the product as viscous oil (0.67 g, 82%). ^1H NMR ($CDCl_3/CD_3OD$): δ 5.76 (s, 1H), 5.36 (br s, 1H), 4.85 (hep, J = 6.0 Hz, 1H), 4.29 (d, J = 6.3 Hz, 2H), 1.45 (s, 9H), 1.36 (d, J = 6.3 Hz, 6H). ^{13}C NMR ($CDCl_3$): δ 170.9, 170.2, 155.5, 93.8, 80.1, 73.2, 37.1, 28.4, 22.8, 22.0, 14.2.

*5-(tert-butyloxycarbonyl)aminomethyl-4-methyl-3-isopropoxyisoxazole (**23**).* A solution of **22** (0.610 g, 2.38 mmol) in dry THF (10 mL) at −78 °C was dropwise added *n*-BuLi (3.3 mL, 1.6 M in THF, 5.23 mmol) and stirring was continued for 45 min at −78 °C. Methyl iodide (0.355 mL, 5.71 mmol) was added and stirring was continued for 2 h at −78 °C. The mixture was quenched with aqueous NH_4Cl (10 mL) and extracted with CH_2Cl_2 (3 × 5 mL). The combined organic phase was dried over $MgSO_4$ and evaporated under vacuum. Purification by DCVC (heptane/EtOAc 4:1) afforded the product as colorless oil (380 mg, 59%). ^1H NMR ($CDCl_3/CD_3OD$): δ 4.94 (br s, 1H), 4.88 (hep, J = 6.3 Hz, 1H), 4.25 (d, J = 6.0 Hz, 2H), 1.86 (s, 3H), 1.44 (s, 9H), 1.37 (d, J = 6.3 Hz, 6H). ^{13}C NMR ($CDCl_3$): δ 170.2, 164.0, 155.4, 102.4, 80.0, 73.1, 35.7, 28.5, 22.1, 5.5.

*4-(Aminomethyl)-5-methyl-isoxazol-1-ol hydrobromide (**24**).* A suspension of **23** (0.300 g, 1.109 mmol) in 33% HBr/AcOH (10 mL) was stirred at 60 °C overnight. The reaction mixture was evaporated under vacuum and purified using prep. HPLC. The purified product was stirred in 33% HBr/AcOH at rt for 5 min and evaporated under vacuum. Recrystallization from MeOH/Et_2O afforded the product as colorless crystals (131 mg, 56%): mp (decomp) > 212 °C. ^1H NMR (D_2O): δ 4.23 (s, 2H), 1.91 (s, 3H). Anal. ($C_5H_8N_2O_2$·HBr) C, H, N.

Pharmacology. *Characterization of **2a-o,16,17,24** in Muscimol Binding.* The binding assay was performed using rat brain synaptic membranes of cortex and the central hemispheres from male SPRD rats with tissue preparation as described in the literature.[48] On the day of the experiment, the membrane preparation was quickly thawed, homogenized in 50 vol of ice-cold buffer (50 mM Tris-HCl buffer, pH 7.4), and centrifuged at 48000*g* for 10 min at 4 °C. This washing step was repeated four times and the final pellet was resuspended in buffer. The assay was carried out in 96-well plates, by incubation of membranes (70−80 μg protein) in 200 μL of buffer, 25 μL of [^3H]muscimol (5 nM final concentration), and 25 μL of test substance in various concentrations, for 60 min at 0 °C. The reaction was terminated by rapid filtration through GF/C filters (Perkin-Elmer Life Sciences), using a 96-well Packard FilterMate cell-harvester, followed by washing with 3 × 250 μL of ice-cold buffer. The dried filters were added Microscint scintillation fluid (Perkin-Elmer Life Sciences), and the amount of filterbound radioactivity was quantified in a Packard TopCount microplate scintillator counter. The experiments were performed in triplicate at least three times for each compound. Nonspecific binding was determined using 1.0 mM GABA. The binding data were analyzed by a nonlinear regression curve-fitting procedure using GraphPad Prism v. 5.04 (GrapPad Software, CA, USA).

Functional Characterization in the FMP Assay. The functional characterization of compounds **2a,b,d,f,h,j,n,o** at $GABA_A$Rs in the FLIPR membrane potential blue assay was performed essentially as described previously.[49] 8 × 10^5 tsA-201 cells were split into a 6 cm tissue culture plate and transfected the following day with a total of 5 μg cDNA using Polyfect (Qiagen, Hilden, Germany). Cells were cotransfected with 1 μg of $\alpha_{1,2,3,5}$-pcDNA3.1, 1 μg of β_2-pcDNA3.1 and 3 μg of γ_{2S}-pCDNA3.1, or transfected with 5 μg of ρ_1-pcDNA3. The following day, cells were split into poly-D-lysine-coated black 96-well plates with clear bottom (BD Biosciences, Bedford, MA). 16−24 h later the medium was aspirated, and the cells were washed with 100 μL of Krebs buffer [140 mM NaCl/4.7 mM KCl/2.5 mM $CaCl_2$/1.2 mM $MgCl_2$/11 mM HEPES/10 mM D-glucose, pH 7.4]. 50 μL of Krebs buffer was added to the wells (in the antagonist experiments, various concentrations of the antagonist were dissolved in the buffer), and then an additional 50 μL of Krebs buffer supplemented with assay dye (1 mg/mL) was added to each well. Then the plate was incubated at 37 °C in a humidified 5% CO_2 incubator for 30 min and assayed in a NOVOstar plate reader (BMG Labtechnologies, Offenburg, Germany) measuring emission [in fluorescence units (FU)] at 560 nm caused by excitation at 530 nm before and up to 1 min after addition of 33 μL of agonist solution. The experiments were performed in duplicate at least three times for each compound at each receptor. EC_{70}−EC_{90} concentrations of GABA were used as agonist in the antagonist experiments. Concentration−response curves for agonists and concentration-inhibition curves for antagonists were constructed based on the difference in the fluorescence units (ΔFU) between the maximal fluorescence recording made before and after addition of agonist obtained for different concentrations of the respective ligands. The curves were generated by nonweighted least-squares fits using the program KaleidaGraph 3.6 (Synergy Software).

Functional Characterization Using Whole-Cell Patch-Clamp Electrophysiology. The electrophysiological characterization of compounds **2a,b,c,d** at $GABA_A$Rs was performed essentially as described previously.[46] HEK 293 cells (ECACC, UK) were split into 35 mm Petri dishes. 18−24 h later, the cells were transfected with either a combination of rat α_1-pCis, β2-pCis, and γ_{2S}-pCis (1:1:2 ratio) or human ρ_1-pCDNA3, and cotransfected with plasmid coding for green fluorescent protein (pGreen Lantern, Life technologies, Paisley, UK) in order to visualize transfected cells. Targefect 293 was used as a DNA carrier according to the manufacturer's protocol (Targeting Systems, CA, USA). The cells were used for whole-cell patch-clamp experiments 40−72 h after transfection. Petri dishes with cells were transferred to the stage of an Axiovert 10 microscope (Zeiss, Germany), and the culture medium was exchanged for extracellular recording solution at room temperature (20−22 °C). The extracellular solution contained (in mM): NaCl 140, KCl 3.5, Na_2HPO_4 1.25, $MgSO_4$ 2, $CaCl_2$ 2, glucose 10, and HEPES 10; pH 7.35. Cells containing green fluorescent protein were visualized with UV light from a HBO 50 lamp (Zeiss, Germany). The cells were approached with micropipets of 1.7−3 MΩ resistance manufactured from 1.5 mm o.d. glass (World Precision Instruments, FA, USA). The intrapipette solution contained (in mM): KCl 140, $MgCl_2$ 1, $CaCl_2$ 1, EGTA 10, MgATP 2, and HEPES 10; pH 7.3. Standard patch-clamp techniques[50] in voltage clamp mode were used to record from neurons in the whole-cell configuration using an EPC-9 amplifier (HEKA, Germany). A clamping potential of −60 mV was used. Series resistance was 65−

dx.doi.org/10.1021/jm301473k | J. Med. Chem. XXXX, XXX, XXX−XXX

80% compensated. Whole-cell currents were analyzed using Pulse software (HEKA, Germany). Extracellular solution containing the agonists was applied using a gravity fed 7-barrelled perfusion pipet (List, Germany), which allowed exchange of the extracellular solution surrounding the recorded neuron with a time constant of ~50 ms. The agonists were applied for 5 s every 1 min. Between the agonist applications, drug-free ABSS was applied from one of the barrels. For the agonist concentration−response relationship the equation:

$$I = I_{max}/(1 + \text{antilog}((\log EC_{50} - A)n_H))$$

was fitted to the experimental data (Graphpad Prism Graphpad Software, CA, USA), where I is the peak membrane current, A the logarithm of the agonist concentration, I_{max} is the maximum peak current that the agonist can induce, EC_{50} is the agonist concentration eliciting 50% of I_{max}, and n_H is the Hill coefficient. Data were described using mean and standard error (S.E.).

Computational Modeling. A novel homology model of the full-length $GABA_{\alpha1\beta2\gamma2}$ receptor was used for all modeling.[16] In short, the receptor model was generated as follows: a structural alignment was generated with the glutamate gated chloride channel (GluCl) from *C. elegans*, (PDB: 3RIF) and the ligand gated ion channel from *E. chrysanthemi* (ELIC), (PDB: 2VL0).[14,51] All sequences for the human glycine receptor α subunits and GABA receptor subunits were subsequently aligned to the sequences of GluCl and ELIC as a profile in Clustal X v. 2.0.12.[52] Model building was performed using Modeler v. 9.7.[53] Ligands for docking were created in their ionized states in Maestro 9.2 followed by conformational searches with MacroModel 9.9 (default settings).[54] The global energy minimum conformations were identified for docking. Ligand docking was accomplished with the induced fit docking (IFD)[54,55] workflow in Maestro v. 9.2 and the XP scoring function.[56] By default the IFD procedure allows residues to adapt to the docked ligand in a 5 Å sphere. Docking was performed both with and without a water molecule in the binding site. The water molecule was placed between the β_2Ser156 and β_2Tyr157 backbone and the aromatic ring of β_2Tyr157 and was able to move during IFD. Docking poses were selected based on mutational data and identification of common interaction patterns in the binding site. Finally, selected ligand poses including an 8 Å sphere were energy minimized to convergence using MacroModel 9.9. This allowed the C-loop to open very slightly and gave rise to less strained poses with better geometry in the binding pocket.

■ ASSOCIATED CONTENT

Supporting Information

Synthesis details, elemental analysis data of new target compounds, HPLC and SFC details, pK_a measurement, X-ray crystal structure analysis, and electrophysiological concentration−response relationship details. This material is available free of charge via the Internet at http://pubs.acs.org.

■ AUTHOR INFORMATION

Corresponding Author

*E-mail: bfr@sund.ku.dk. Phone (+45)35336495.

Notes

The authors declare no competing financial interest.

■ ACKNOWLEDGMENTS

We thank Flemming Hansen for technical assistance with collection of X-ray data, Ulla Geneser for technical laboratory assistance, Peter Brøsen for SFC purification and Erling B. Olsen for p*K*a determination. J.G.P. was supported by the Lundbeck Foundation, R.B. was supported by the Velux Foundation, U.K. was supported by the Carlsberg Foundation, and A.A.J. was supported by the Novo Nordisk and Carlsberg Foundations.

■ ABBREVIATIONS:

4-AHP, 4-(aminomethyl)-1-hydroxypyrazole; 4-PHP, 4-(piperidin-4-yl)-1-hydroxypyrazole; 4-PIOL, 5-(4-piperidyl)-3-isoxazol; DCVC, dry column vacuum chromatography; ELIC, *Erwinia* ligand-gated ion channel; FC, flash chromatography; FLIPR, fluorescent imaging plate reader; FMP, FLIPR membrane potential; GABA, γ-aminobutyric acid; GluCl, glutamate-gated chloride channel; IFD, induced fit docking; MW, microwave; RP-FC, reverse phase flash chromatography; SFC, supercritical flash chromatography; THIP, 4,5,6,7-tetrahydroisoxazolo[5,4-*c*]pyridine-3-ol

■ REFERENCES

(1) Foster, A. C.; Kemp, J. A. Glutamate- and GABA-based CNS therapeutics. *Curr. Opin. Pharmacol.* **2006**, *6*, 7−17.

(2) Johnston, G. A. R. $GABA_A$ Receptor Channel Pharmacology. *Curr. Pharm. Des.* **2005**, *11*, 1867.

(3) Dougherty, D. A. Cys-Loop Neuroreceptors: Structure to the Rescue? *Chem. Rev.* **2008**, *108*, 1642−1653.

(4) Paul, J, W. $GABA_A$ receptor subtypes in the brain: a paradigm for CNS drug discovery? *Drug Discovery Today* **2003**, *8*, 445−450.

(5) Sieghart, W. Structure, Pharmacology, and Function of $GABA_A$ Receptor Subtypes. In *Adv. Pharmacol.*; Enna, S. J., Ed.; Academic Press: New York, 2006; Vol. *54*, pp 231−263.

(6) Johnston, G. A. R.; Curtis, D. R.; de Groat, W. C.; Duggan, A. W. Central actions of ibotenic acid and muscimol. *Biochem. Pharmacol.* **1968**, *17*, 2488−2489.

(7) Krogsgaard-Larsen, P.; Johnston, G. A. R.; Lodge, D.; Curtis, D. R. A new class of GABA agonist. *Nature* **1977**, *268*, 53−55.

(8) Ebert, B.; Wafford, K. A.; Whiting, P. J.; Krogsgaard-Larsen, P.; Kemp, J. A. Molecular pharmacology of gamma-aminobutyric acid type A receptor agonists and partial agonists in oocytes injected with different alpha, beta, and gamma receptor subunit combinations. *Mol. Pharmacol.* **1994**, *46*, 957−963.

(9) Brown, N.; Kerby, J.; Bonnert, T. P.; Whiting, P. J.; Wafford, K. A. Pharmacological characterization of a novel cell line expressing human $\alpha_4\beta_3\delta$ $GABA_A$ receptors. *Br. J. Pharmacol.* **2002**, *136*, 965−974.

(10) Kristiansen, U.; Lambert, J. D. C.; Falch, E.; Krogsgaard-Larsen, P. Electrophysiological studies of the GABAA receptor ligand, 4-PIOL, on cultured hippocampal neurones. *Br. J. Pharmacol.* **1991**, *104*, 85−90.

(11) Byberg, J. R.; Labouta, I. M.; Falch, E.; Hjeds, H.; Krogsgaard-Larsen, P. Synthesis and biological activity of a $GABA_A$ agonist which has no effect on benzodiazepine binding and of structurally related glycine antagonists. *Drug Des. Delivery* **1987**, *1*, 261−274.

(12) Frølund, B.; Jørgensen, A. T.; Tagmose, L.; Stensbøl, T. B.; Vestergaard, H. T.; Engblom, C.; Kristiansen, U.; Sanchez, C.; Krogsgaard-Larsen, P.; Liljefors, T. Novel Class of Potent 4-Arylalkyl Substituted 3-Isoxazolol $GABA_A$ Antagonists: Synthesis, Pharmacology, and Molecular Modeling. *J. Med. Chem.* **2002**, *45*, 2454−2468.

(13) Frølund, B.; Tagmose, L.; Liljefors, T.; Stensbøll, T. B.; Engblom, C.; Kristiansen, U.; Krogsgaard-Larsen, P. A Novel Class of Potent 3-Isoxazolol $GABA_A$ Antagonists: Design, Synthesis, and Pharmacology. *J. Med. Chem.* **2000**, *43*, 4930−4933.

(14) Hibbs, R. E.; Gouaux, E. Principles of activation and permeation in an anion-selective Cys-loop receptor. *Nature* **2011**, *474*, 54−60.

(15) Sander, T.; Frølund, B.; Bruun, A. T.; Ivanov, I.; McCammon, J. A.; Balle, T. New insights into the $GABA_A$ receptor structure and orthosteric ligand binding: Receptor modeling guided by experimental data. *Proteins: Struct., Funct., Bioinf.* **2011**, *79*, 1458−1477.

(16) Bergmann, R.; Kongsbak, K.; Sørensen, P. L.; Sander, T.; Balle, T. A Unified model of the $GABA_A$ receptor comprising agonist and benzodiazepine binding sites. *PLoS ONE 8*, e52323, doi: 10.1371.

(17) Møller, H. A.; Sander, T.; Kristensen, J. L.; Nielsen, B.; Krall, J.; Bergmann, M. L.; Christiansen, B.; Balle, T.; Jensen, A. A.; Frølund, B. Novel 4-(Piperidin-4-yl)-1-hydroxypyrazoles as γ-Aminobutyric $Acid_A$

Receptor Ligands: Synthesis, Pharmacology, and Structure-Activity Relationships. *J. Med. Chem.* **2010**, *53*, 3417−3421.
(18) Felding, J.; Kristensen, J.; Bjerregaard, T.; Sander, L.; Vedsø, P.; Begtrup, M. Synthesis of 4-Substituted 1-(Benzyloxy)pyrazoles via Iodine-Magnesium Exchange of 1-(Benzyloxy)-4-iodopyrazole. *J. Org. Chem.* **1999**, *64*, 4196−4198.
(19) Caddick, S.; Judd, D. B.; Lewis, A. K. d. K.; Reich, M. T.; Williams, M. R. V. A generic approach for the catalytic reduction of nitriles. *Tetrahedron* **2003**, *59*, 5417−5423.
(20) Caddick, S.; de K. Haynes, A. K.; Judd, D. B.; Williams, M. R. V. Convenient synthesis of protected primary amines from nitriles. *Tetrahedron Lett.* **2000**, *41*, 3513−3516.
(21) Vedsø, P.; Begtrup, M. Synthesis of 5-Substituted 1-Hydroxypyrazoles through Directed Lithiation of 1-(Benzyloxy)-pyrazole. *J. Org. Chem.* **1995**, *60*, 4995−4998.
(22) Dreher, S. D.; Lim, S.-E.; Sandrock, D. L.; Molander, G. A. Suzuki-Miyaura Cross-Coupling Reactions of Primary Alkyltrifluoroborates with Aryl Chlorides. *J. Org. Chem.* **2009**, *74*, 3626−3631.
(23) Young, J. F.; Osborn, J. A.; Jardine, F. H.; Wilkinson, G. Hydride intermediates in homogeneous hydrogenation reactions of olefins and acetylenes using rhodium catalysts. *Chem. Commun. (London)* **1965**, 131−132.
(24) Xia, N.; Taillefer, M. A Very Simple Copper-Catalyzed Synthesis of Anilines by Employing Aqueous Ammonia. *Angew. Chem., Int. Ed.* **2009**, *48*, 337−339.
(25) Molander, G. A.; Hiebel, M.-A. Synthesis of Amidomethyltrifluoroborates and Their Use in Cross-Coupling Reactions. *Org. Lett.* **2011**, *12*, 4876−4879.
(26) Molander, G. A.; Shin, I. Suzuki-Miyaura Cross-Coupling Reactions of Potassium Boc-Protected Aminomethyltrifluoroborate with Aryl and Hetaryl Mesylates. *Org. Lett.* **2012**, *14*, 3138−3141.
(27) Fukui, H.; Inoguchi, K.; Nakano, J. Synthesis of the Bicyclic Secondary Amines *via* Dimethylaminomethylene Ketones from 3-Pyrrolidone and 4-Piperidone. *Heterocycles* **2002**, *56*, 257−264.
(28) Begtrup, M.; Vedsø, P. Preparation of *N*-hydroxyazoles by oxidation of azoles. *J. Chem. Soc., Perkin Trans. 1* **1995**, 243−247.
(29) CCDC 901038 contains the supplementary crystallographic data for this paper. These data can be obtained free of charge via www.ccdc.cam.ac.uk/data_request/cif, or by emailing data_request@ccdc.cam.ac.uk, or by contacting The Cambridge Crystallographic Data Centre, 12, Union Road, Cambridge CB2 1EZ, UK; fax: +44 1223 336033.
(30) Krogsgaard-Larsen, P.; Larsen, A. L. N.; Thyssen, K. GABA Receptor Agonists. Synthesis of Muscimol Analogues Including (*R*)- and (*S*)-5-(1-Aminoethyl)-3-isoxazolol and (*RS*)-5-Aminomethyl-2-isoxazolin-3-ol. *Acta Chem. Scand.* **1978**, *B32*, 469−477.
(31) Frey, M.; Jäger, V. Synthesis of N-Substituted Muscimol Derivatives Including N-Glycylmuscimol. *Synthesis* **1985**, *1100*, 1104.
(32) Vogensen, S. B.; Clausen, R. P.; Greenwood, J. R.; Johansen, T. N.; Pickering, D. S.; Nielsen, B.; Ebert, B.; Krogsgaard-Larsen, P. Convergent Synthesis and Pharmacology of Substituted Tetrazolyl-2-amino-3-(3-hydroxy-5-methyl-4-isoxazolyl)propionic acid Analogues. *J. Med. Chem.* **2005**, *48*, 3438−3442.
(33) Wenckens, M.; Jakobsen, P.; Vedsø, P.; Huusfeldt, P. O.; Gissel, B.; Barfoed, M.; Lundin Brockdorff, B.; Lykkesfeldt, A. E.; Begtrup, M. N-Alkoxypyrazoles as biomimetics for the alkoxyphenyl group in tamoxifen. *Bioorg. Med. Chem.* **2003**, *11*, 1883−1899.
(34) Jørgensen, C. G.; Bräuner-Osborne, H.; Nielsen, B.; Kehler, J.; Clausen, R. P.; Krogsgaard-Larsen, P.; Madsen, U. Novel 5-substituted 1-pyrazolol analogues of ibotenic acid: Synthesis and pharmacology at glutamate receptors. *Bioorg. Med. Chem.* **2007**, *15*, 3524−3538.
(35) Stensbøl, T. B.; Uhlmann, P.; Morel, S.; Eriksen, B. L.; Felding, J.; Kromann, H.; Hermit, M. B.; Greenwood, J. R.; Braüner-Osborne, H.; Madsen, U.; Junager, F.; Krogsgaard-Larsen, P.; Begtrup, M.; Vedsø, P. Novel 1-Hydroxyazole Bioisosteres of Glutamic Acid. Synthesis, Protolytic Properties, and Pharmacology. *J. Med. Chem.* **2001**, *45*, 19−31.
(36) Clausen, R. P.; Christensen, C.; Hansen, K. B.; Greenwood, J. R.; Jørgensen, L.; Micale, N.; Madsen, J. C.; Nielsen, B.; Egebjerg, J.; Bräuner-Osborne, H.; Traynelis, S. F.; Kristensen, J. L. N-Hydroxypyrazolyl Glycine Derivatives as Selective N-Methyl-d-aspartic Acid Receptor Ligands. *J. Med. Chem.* **2008**, *51*, 4179−4187.
(37) Frølund, B.; Jensen, L. S.; Guandalini, L.; Canillo, C.; Vestergaard, H. T.; Kristiansen, U.; Nielsen, B.; Stensbøl, T. B.; Madsen, C.; Krogsgaard-Larsen, P.; Liljefors, T. Potent 4-Aryl- or 4-Arylalkyl-Substituted 3-Isoxazolol $GABA_A$ Antagonists: Synthesis, Pharmacology, and Molecular Modeling. *J. Med. Chem.* **2004**, *48*, 427−439.
(38) Frølund, B.; Jensen, L. S.; Storustovu, S. I.; Stensbøl, T. B.; Ebert, B.; Kehler, J.; Krogsgaard-Larsen, P.; Liljefors, T. 4-Aryl-5-(4-Piperidyl)-3-Isoxazolol $GABA_A$ Antagonists: Synthesis, Pharmacology, and Structure-Activity Relationships. *J. Med. Chem.* **2007**, *50*, 1988−1992.
(39) Krogsgaard-Larsen, P.; Johnston, G. A. R. Structure-Activity Studies on the Inhibition of GABA Binding to Rat Brain Membranes by Muscimol and Related Compounds. *J. Neurochem.* **1978**, *30*, 1377−1382.
(40) Haefliger, W.; Révész, L.; Maurer, R.; Römer, D.; Büscher, H.-H. Synthesis and structure-activity studies on analogues and derivatives of muscimol and THIP. *Chim. Ther* **1984**, *19*, 149−156.
(41) Krogsgaard-Larsen, P.; Hjeds, H.; Curtis, D. R.; Lodge, D.; Johnston, G. A. R. Dihydromuscimol, thiomuscimol, and related heterocyclic compounds as GABA analogues. *J. Neurochem.* **1979**, *32*, 1717−1724.
(42) Hansen, S. B.; Sulzenbacher, G.; Huxford, T.; Marchot, P.; Taylor, P.; Bourne, Y. Structures of Aplysia AChBP complexes with nicotinic agonists and antagonists reveal distinctive binding interfaces and conformations. *EMBO J.* **2005**, *24*, 3635−3646.
(43) Graham, A. R. J.; Mary, C.; Jane, R. H.; Kenneth, N. M. $GABA_C$ Receptors as Drug Targets. *Curr. Drug Targets: CNS Neurol. Disord.* **2003**, *2*, 260−268.
(44) Lummis, S. C. R.; L. Beene, D.; Harrison, N. J.; Lester, H. A.; Dougherty, D. A. A Cation-π Binding Interaction with a Tyrosine in the Binding Site of the $GABA_C$ Receptor. *Chem. Biol.* **2005**, *12*, 993−997.
(45) Padgett, C. L.; Hanek, A. P.; Lester, H. A.; Dougherty, D. A.; Lummis, S. C. R. Unnatural Amino Acid Mutagenesis of the $GABA_A$ Receptor Binding Site Residues Reveals a Novel Cation−π Interaction between GABA and β_2Tyr97. *J. Neurosci.* **2007**, *27*, 886−892.
(46) Madsen, C.; Jensen, A. A.; Liljefors, T.; Kristiansen, U.; Nielsen, B.; Hansen, C. P.; Larsen, M.; Ebert, B.; Bang-Andersen, B.; Krogsgaard-Larsen, P.; Frølund, B. 5-Substituted Imidazole-4-acetic Acid Analogues: Synthesis, Modeling, and Pharmacological Characterization of a Series of Novel γ-Aminobutyric $Acid_C$ Receptor Agonists. *J. Med. Chem.* **2007**, *50*, 4147−4161.
(47) Pedersen, D. S.; Rosenbohm, C. Dry Column Vacuum Chromatography. *Synthesis* **2001**, 2431−2434.
(48) Ransom, R. W.; Stec, N. L. Cooperative Modulation of [3H]MK-801 Binding to the N-Methyl-d-Aspartate Receptor-Ion Channel Complex by l-Glutamate, Glycine, and Polyamines. *J. Neurochem.* **1988**, *51*, 830−836.
(49) Jensen, A. A.; Bergmann, M. L.; Sander, T.; Balle, T. Ginkgolide X Is a Potent Antagonist of Anionic Cys-loop Receptors with a Unique Selectivity Profile at Glycine Receptors. *J. Biol. Chem.* **2010**, *285*, 10141−10153.
(50) Hamill, O. P.; Marty, A.; Neher, E.; Sakmann, B.; Sigworth, F. J. Improved patch-clamp techniques for high-resolution current recording from cells and cell-free membrane patches. *Pflüg. Arch. Eur. J. Phys.* **1981**, *391*, 85−100.
(51) Hilf, R. J. C.; Dutzler, R. X-ray structure of a prokaryotic pentameric ligand-gated ion channel. *Nature* **2008**, *452*, 375−379.
(52) Larkin, M. A.; Blackshields, G.; Brown, N. P.; Chenna, R.; McGettigan, P. A.; McWilliam, H.; Valentin, F.; Wallace, I. M.; Wilm, A.; Lopez, R.; Thompson, J. D.; Gibson, T. J.; Higgins, D. G. Clustal W and Clustal X version 2.0. *Bioinformatics* **2007**, *23*, 2947−2948.
(53) Sali, A.; Blundell, T. L. Comparative Protein Modelling by Satisfaction of Spatial Restraints. *J. Mol. Biol.* **1993**, *234*, 779−815.

(54) *MacroModel*, version 9.9, Schrödinger, LLC, New York, NY, 2011.
(55) *Jaguar*, version 7.8, Schrödinger, LLC, New York, NY, 2011.
(56) Friesner, R. A.; Murphy, R. B.; Repasky, M. P.; Frye, L. L.; Greenwood, J. R.; Halgren, T. A.; Sanschagrin, P. C.; Mainz, D. T. Extra Precision Glide: Docking and Scoring Incorporating a Model of Hydrophobic Enclosure for Protein-Ligand Complexes. *J. Med. Chem.* **2006**, *49*, 6177−6196.
(57) Lolli, M. L.; Hansen, S. L.; Rolando, B.; Nielsen, B.; Wellendorph, P.; Madsen, K.; Larsen, O. M.; Kristiansen, U.; Fruttero, R.; Gasco, A.; Johansen, T. N. Hydroxy-1,2,5-oxadiazolyl Moiety as Bioisoster of the Carboxy Function. Synthesis, Ionization Constants, and Pharmacological Characterization of γ-Aminobutyric Acid (GABA) Related Compounds. *J. Med. Chem.* **2006**, *49*, 4442−4446.
(58) Ebert, B.; Frølund, B.; Diemer, N. H.; Krogsgaard-Larsen, P. Equilibrium binding characteristics of [^{3}H]thiomuscimol. *Neurochem. Int.* **1999**, *34*, 427−434.
(59) Krehan, D.; Frølund, B.; Ebert, B.; Nielsen, B.; Krogsgaard-Larsen, P.; Johnston, G. A. R.; Chebib, M. Aza-THIP and related analogues of THIP as $GABA_C$ antagonists. *Bioorg. Med. Chem.* **2003**, *11*, 4891−4896.